The Surface and Subsurface Distribution and Transport of Sodium within a Constructed Fen Peatland in a Post-Mined Landscape in the Alberta Oil Sands Region

by

Suyuan Yang

A thesis
presented to the University of Waterloo
in fulfillment of the
thesis requirement for the degree of
Master of Science
in
Geography

Waterloo, Ontario, Canada, 2021

Author's Declaration

I hereby declare that I am the sole author of this thesis. This is a true copy of the thesis, including any required final revisions, as accepted by my examiners.

I understand that my thesis may be made electronically available to the public.

Abstract

Nikanotee Fen Watershed is an engineered upland-fen peatland system in the Athabasca Oil Sands Region constructed from salvaged peat and forest soils, overburden and tailings sand materials. Sodium-rich leachate from tailings sand has been shown to migrate to the fen system through groundwater, as expected, where it impacts fen vegetation health. The goal of this research is to quantify the spatial distribution of EC (electrical conductivity) and sodium (Na^+) in ponded surface water and in the shallow subsurface zone (top 35 cm) of the fen peat deposit. Water samples collected from the ponded surface water and subsurface zone (10 and 30 cm below ground surface (bgs), with 5 and 10 cm intake, respectively) of the fen in 2019 showed that seasonal average Na^+ concentration and EC were ~290 mg L^{-1} and ~2800 µS cm^{-1}, respectively. The highest Na^+ concentration and EC were generally found in the wettest part of the fen (southwest corner; average water table 16 cm above ground surface (ags)), and the lowest were found in the relatively dry (average water table 1.5 cm bgs) north-east corner near the drainage outlet of the fen. Na^+ concentration and EC in ponded surface water were more responsive to precipitation dilution and evapotranspiration concentration, whereas in the subsurface zone, they were steadier, but generally increased from May to August. The change in Na^+ mass measured between June 3rd and August 13th in ponded surface water and in the shallow subsurface (0-35 cm) of the fen (-66 kg) was smaller than that estimated from the sum of hydrologically driven fluxes (groundwater inflow and fen discharge; atmospheric fluxes were negligible), which was -179 kg (i.e., a net loss over this period). The 2019 season (May to August) was relatively wet and cool, with 264 mm precipitation input, 272 mm actual evapotranspiration output, 61 mm fen runoff output, 26 mm groundwater inflow, with average air temperature of 14 °C. The water budget showed a net loss, but storage change showed an increase, which could be the uncertainty that arises with groundwater underestimation. The precipitation-driven discharge controlled the mass efflux of Na^+ from the system at an estimated seasonal average rate of 4 kg day^{-1} (total of 261 kg from June to August) with an average Na^+ concentration of 229 ± 148 mg L^{-1}. At the rate of Na^+ discharge observed in 2019, the residence time of the original Na^+ mass in the fen and upland system (27 tonnes) was estimated to be 36 frost-free seasons (183 days per year) post-construction under similar wet and cool weather conditions. Given the relatively small proportion of salt being flushed annually, elevated levels of salinity will likely be sustained for several decades. Na^+ has reached the rooting zone, so salt-tolerant vegetation is an important attribute that should be targeted for newly constructed systems. Monitoring Na^+ concentration and EC in discharge more frequently and for a longer period is recommended to refine the flushing timeframe prediction.

Acknowledgements

Graduate studies have been a challenging but rewarding journey. I am so glad to have the opportunity to be part of the Wetland's Hydrology Research Lab. I am truly grateful to my supervisor, Dr. Jonathan Price, for the invaluable advice and guidance you provided throughout this journey. Your insightful feedback pushed me to sharpen my thinking and brought my work to a higher level.

I would like to thank everyone in the Wetland's Hydrology Research Lab and the Fort McMurray research crew for their support in the field and acceptance to the sweets I baked when I felt stressed. Special thanks to Emily Prystupa, Kimberly Tran, Jacob Whitehouse, Gabriel Dubé, and Janet Hu for all their help in the field. The help with the laboratory analysis, writing, or general advice from Eric Kessel, Janina Plach, Owen Sutton, Nicole Balliston, and James Sherwood is much appreciated. I would also like to thank my committees Dr. Scott Ketcheson and Matthew Elmes for contributing edits to the final thesis draft.

Thank you to the Suncor Field Service's and Reclamation teams and Bear Scare for their assistance. Funding for this project was provided by an NSERC CRD grant and co-funded by Suncor Energy Inc., Imperial Oil Resources Limited and Teck Resources Limited.

I would like to thank everyone who has contributed in one way or other along my journey. To my friends here and back home, thank you for your patience and encouragement during the periods of self-doubt. To my mum and dad, thank you for always encouraging me and keeping me motivated. I am fortunate to have your continuous support. Lastly, to my cats, thanks for keeping me company and making me smile all the time.

Land Acknowledgement

I would like to acknowledge that my project's lab work and desk work takes place on the traditional territory of the Neutral, Anishinaabe, and Haudenosaunee Peoples. The University of Waterloo is situated on the Haldimand Tract, land promised to Six Nations, which includes six miles on each side of the Grand River. I would like to acknowledge that my project's field research takes place within the boundaries of Treaty 8, traditional lands of the Dene and Cree, as well as the traditional lands of the Métis of northeastern Alberta.

I understand that in both these regions Indigenous Peoples have been stewards of the land long before I began my research and have thus accumulated knowledge of the lands and waters on which they have lived and currently live.

Table of Contents

Author's Declaration ii
Abstract iii
Acknowledgements iv
List of Figures vii
List of Tables x
List of Abbreviations xi
Chapter 1 Introduction 1
1.1 Background 1
1.2 Hypotheses 2
1.3 Study site 3
Chapter 2 Methods 6
2.1 Hydrometeorological analyses and water balance 6
2.2 Surface and groundwater sampling 7
2.2.1 Location of surface and subsurface sampling points 8
2.2.2 Lysimeter porewater extraction 9
2.2.3 V-notch and spill box 10
2.2.4 Hillslopes 12
2.3 Na^+ concentrations and validation 12
2.4 Statistical analyses 13
2.5 Surfer interpolation 13
2.6 Mass balance 14
2.6.1 Na^+ mass measured in ponded surface water and subsurface peat 14
2.6.2 Na^+ mass in fluxes 17
Chapter 3 Results 19
3.1 Hydrometeorology 19
3.2 Na^+ concentrations and EC distribution 23
3.3 Spatial interpolation and temporal patterns 26
3.4 Mass balance 34
3.4.1 Additional Na^+ mass estimation 36
Chapter 4 Discussion 37
4.1 Hydrological pathways for Na^+ 37
4.2 Na^+ mass balance comparison 39

4.3 Potential sources of errors 41
Chapter 5 Conclusion 43
Bibliography 46
Appendix 50
Appendix A Sodium probe validation 50
Appendix B Estimation for Na^+ concentrations in surface ponded water 51
Appendix C Validation for Na^+ concentrations in discharge 54
Appendix D Hydrological context in past years 56
Appendix E Calculation process for dilution at ponded surface water 57
Appendix F Na^+ mass estimate in peat 58
Appendix G Additional violin plots with statistical test for each sampling events 59
Appendix H Limitations and gap-fills for groundwater inflow of Na^+ estimation 61
Appendix I Vertical hydraulic gradient 62

List of Figures

Figure 1-1 Map of Nikanotee Fen with site instrumentation and layer properties (retrieved from Kessel et al. 2018). Cross-section (bottom) illustrates the layering of materials and groundwater flow lines of particles dropped as an equal distance along the water table. The red dots showed the locations of runoff flume on each hillslope (southeast, east, and west). 4

Figure 1-2 (a) Map of Nikanotee Fen with locations of sampled points (dark blue circles for ponded surface water, yellow diamonds for pore water from suction lysimeters at 10 and 30 cm bgs, green triangles for pore water from piezometers at 30 cm bgs) and ponded water (light blue shaded areas). The box with an "x" indicates the location of the spill box that redirects discharge out of the watershed. (b) Topography of the fen, collected in 2015. The observed ponded water area in 2019 matches with the areas with lower elevations in the fen. 5

Figure 2-1 Photo of a piezometer at 30 cm bgs and adjacent ponded surface water, located at the north west corner of the fen. 9

Figure 2-2 Photo of two suction lysimeters installed at 30 cm bgs (left, with white tape) and 10 cm bgs (right, with yellow tape) in a ponded area. 10

Figure 2-3 Photos of v-notch and ISCO auto sampler. (a) an overview of the outflow setup, with ISCO auto sampler on the right. (b) a close-up view of the ISCO auto sampler collecting water from behind the v-notch. Blue arrows indicate the outflow direction. 11

Figure 2-4 Runoff flume installed on the east slope. (a) one end of the flume was instrumented with sample bottle attached to collect runoff water sample. A pressure transducer installed in the bucket was used to estimate flow. (b) flow-collector above the flume, sealed with hydraulic cement. 12

Figure 2-5 Simplified fen cells for sodium mass storage estimation. 14 cells were used in this model, with conceptual water table to demonstrate unsaturated and saturated zones of peat. (a) the plan view of the conceptual model with sample point locations in the fen. (b) the 3-D view of the conceptual model of 0 ~ 35 cm of peat. (c) a simplified example of a single fen cell with half dry surface with unsaturated peat, and half ponded surface water on top of the peat containing one piezometer at 30 cm bgs. 15

Figure 2-6 Conceptual cross-section diagram of volumes calculated using Grid Volume command (not to scale). The top figure is when lower surface is set as a constant z = 0 and the bottom figure is when lower surface is set as the bottom boundary of this study (top 35 cm peat, when z = -35). 16

Figure 2-7 Conceptual salt budget model (not to scale), demonstrating flow lines (red lines) and potential pathways for Na^+ movement (blue arrows). 18
Figure 3-1 Summary of field data collected between May 18th and August 31st, 2019 including: (a) *P*; (b) water table, Na^+ concentrations and EC measured from ponded surface water, 10 and 30 cm bgs, and their daily averages; and (c) discharge, Na^+ concentrations and EC in discharge (Na^+ concentrations estimated and validated with calibrated EC measured by HOBO). Here, frozen period contains data collected in May, the dry period starts from June 1st to just before the largest rainfall event on June 28th, and the wet period includes data collected from June 28th to the end of August. 21
Figure 3-2 (a) bar plot of *P* and *AET* with cumulative *P* – *AET* line and discharge line; (b) summary table of *P*, *AET*, and *Q* (with respect to the fen area, 2.9 ha) within every sample events intervals (grey shaded); (c) violin plots of Na^+ concentrations within ponded surface water (surf), 10 cm bgs (z10) and 30 cm bgs (z30) from each sample events; (d) violin plots for EC within surf, z10 and z30 from each sample events. A violin plot is hybrid of a box plot in the center, which shows the median, interquartile range (first and third quartile), lower/upper adjacent values, and outliers; and a kernel density estimate, which is a non-parametric depiction of the probability density function (Hintze & Nelson, 1998). *samples collected on these dates were excluded for mass balance calculation. 22
Figure 3-3 Average ± 1 Standard Deviation of Na^+ concentration and EC by depth below ground surface in fen peat. 24
Figure 3-4 Seasonal Na^+ (a) and EC (b) measured from ponded surface water (surf), 10 cm bgs (z10) and 30 cm bgs (z30) using Wilcoxon rank sum test ($\alpha = 0.05$) for pairwise comparisons. Note that ns means not significant at any level equal to 0.05 or higher, whereas *, **, *** and **** indicate significance at $p<0.05$, 0.01, 0.001 and 0.0001, respectively. 25
Figure 3-5 Na^+ (a) and EC (b) by category including ponded surface water (surf), 10 cm bgs (z10) and 30 cm bgs (z30) and tested difference between dry and wet periods as previously defined. Note that ns indicates not significant, whereas *, **, ***, and **** indicate significance at 0.05, 0.01, 0.001 and 0.0001, respectively. 25
Figure 3-6 Water table height contours in cm relative to ground surface shown for a dry period (May to June) and a wet period (July to August). 27

Figure 3-7 Spatial distribution of sodium concentrations interpolation in surface water at Nikanotee Fen, 2019. May and June were considered as dry period; July and August were considered as wet period. 28
Figure 3-8 Spatial distribution of sodium concentrations at 10 cm bgs in Nikanotee Fen, May 29th – August 13th, 2019. 29
Figure 3-9 Spatial distribution of sodium concentration at 30 cm bgs in Nikanotee Fen, 29th – August 13th, 2019. 30
Figure 3-10 Spatial distribution of EC in ponded surface water at Nikanotee Fen, 29th – August 13th, 2019. 31
Figure 3-11 Spatial distribution of EC at 10 cm bgs in Nikanotee Fen, 29th – August 13th, 2019. 32
Figure 3-12 Spatial distribution of EC at 30 cm bgs in Nikanotee Fen, 29th – August 13th, 2019. 33
Figure 3-13 Na^+ mass (kg) estimated in ponded surface water layer (Na^+ water), unsaturated peat layer (Na^+ unsat) and saturated peat layer (Na^+ sat), for the zone above 35 cm bg, for each sampling events. 35

List of Tables

Table 3-1 Hydrological and water balance components for 2019, including precipitation *P*, actual evapotranspiration *AET* (potential evapotranspiration *PET*), fen runoff *q*, groundwater flux *GW*, change in storage $\Delta \boldsymbol{S}$, water balance residual ε, and average air temperature *T*. Units in mm unless specified. 19

Table 3-2 Mean Na^+ concentrations and EC (± Standard Deviation) within ponded surface water and subsurface peat, from frozen, dry, and wet period. Bolded values denote the highest average of all periods. 24

Table 3-3 Seasonal mean Na^+ concentrations and EC (± Standard Deviation) within peat, from ponded surface water (surf), 10 cm bg (z10), 30 cm bgs (z30), 50 cm bgs (z50) surface discharge at v-notch (ISCO), and discharge at spill box (SB). Sample numbers ranged from 11 to 2396 for each category. 24

Table 3-4 Seasonal average of volume ($\boldsymbol{V}$), Na^+ concentrations ($\boldsymbol{C}$), and volumetric water content ($\boldsymbol{\theta}$), measured in the field during the study period, with porosity previously measured by Kessel et al. (2018). 34

Table 3-5 Sodium mass estimation for each sampling events (unit in kg) 34

List of Abbreviations

AET	…….	Actual evapotranspiration (mm)
A	…….	Area (m^2 or ha)
A_{peat}	…….	Area of the peat, equivalent to the total cell area (m^2)
AOSR	…….	Alberta Oil Sand Region
ags	…….	Above ground surface
bgs	…….	Below ground surface
b_{peat}	…….	Thickness of the peat (m)
C_1	…….	Na^+ concentration in ponded surface water on day 1 (mg L^{-1})
C_2	…….	Na^+ concentration in ponded surface water on day 2 (mg L^{-1})
C_{peat}	…….	Average Na^+ concentration at level 50, 90 and 150 cm bgs (mg L^{-1})
C_{sat}	…….	Na^+ concentration of saturated peat (mg L^{-1})
C_{unsat}	…….	Na^+ concentration of unsaturated peat (mg L^{-1})
C_{water}	…….	Na^+ concentration of ponded surface water (mg L^{-1})
C_{AET}	…….	Na^+ concentration in actual evapotranspiration (mg L^{-1})
C_{Dionex}	…….	Na^+ concentration measured by Dionex (mg L^{-1})
C_{Orion}	…….	Na^+ concentration measured by Orion probe (mg L^{-1})
C_{GW}	…….	Na^+ concentration in groundwater (mg L^{-1})
C_P	…….	Na^+ concentration in precipitation (mg L^{-1})
C_Q	…….	Na^+ concentration in discharge (mg L^{-1})
C_R	…….	Na^+ concentration in hillslope runoff (mg L^{-1})
ΔM	…….	Total Na^+ mass estimated in fluxes from June 3rd to August 13th (kg)
ΔM_{water}	…….	Na^+ mass change in storage in the ponded surface water (kg)
ΔNa_{Tot}	…….	Total Na^+ mass change in storage from June 3rd to August 13th (kg)
ΔS	…….	Change in storage (mm)
ΔWT_{ags}	…….	Change in water table above ground surface (mm)
ΔWT_{bgs}	…….	Change in water table below ground surface (mm)
DOC	…….	Dissolved organic carbon
DOY	…….	Day of the year
ε	…….	Error term

EC	…….	Electrical conductivity (μS cm^{-1})
GW	…….	Groundwater flux (mm)
h_{well}	…….	Head measured in well (m)
h_{z225}	…….	Head measured in piezometer centered at 225 cm bgs (m)
i_{vert}	…….	Vertical hydraulic gradient
ISA	…….	Ionic strength adjuster
K_{sat}	…….	Peat saturated hydraulic conductivity (m $year^{-1}$)
$l_{z225} - l_{well}$	…….	Distance between water table and the mid screen of the piezometer centered at 225 cm bgs (m)
LFH	…….	Litter, Fermentation, Humus
M_1	…….	Na^+ mass estimated in ponded surface water on day 1 (kg)
M_2	…….	Na^+ mass estimated in ponded surface water on day 2 (kg)
M_{GW}	…….	Na^+ mass found in groundwater flux (kg)
M_Q	…….	Na^+ mass found in discharge (kg)
mASL	…….	Meter above sea level
n	…….	Number of neighboring data values
Na_{sat}	…….	Na^+ mass in saturated peat (top 35 cm) (kg)
Na_{Tot}	…….	Total Na^+ mass contained in the ponded surface water and in the top 35 cm of peat (kg)
Na_{unsat}	…….	Na^+ mass in unsaturated peat (kg)
Na_{water}	…….	Na^+ mass in ponded surface water (kg)
Na^+	…….	Sodium ion
P	…….	Precipitation (mm)
PET	…….	Potential evapotranspiration (mm)
q	…….	Fen runoff at the v-notch (mm)
Q	…….	Discharge (L s^{-1})
R	…….	Hillslope runoff (mm)
SB	…….	Spill box
surf	…….	Ponded surface water
S_y	…….	Specific yield
T	…….	Temperature (°C)

V	…….	Volume (m^3)
V_1	…….	Volume of ponded surface water on day 1 (m^3)
V_d	…….	Volume of freshwater added to the ponded surface to dilute from C_1 to C_2 (m^3)
V_{-35}	…….	Positive volume above z = -35 extracted from Surfer (m^3)
V_{sat}	…….	Volume of saturated peat (top 35 cm) (m^3)
V_{unsat}	…….	Volume of unsaturated peat (m^3)
V_{water}	…….	Volume of ponded surface water (m^3)
W_i	…….	Weight of the value at location i
WT	…….	Water table (cm)
z10	…….	Suctions lysimeter centered at 10 cm bgs
z30	…….	Piezometer or suctions lysimeter centered at 30 cm bgs
Z_A	…….	Estimated value of grid node A
Z_i	…….	Value at location i
θ	…….	Volumetric water content

Chapter 1
Introduction

1.1 Background

With the increasing demand for oil from rapid industrialization, the oil sand extraction in Alberta has disturbed approximately 953 km^2 of land area by open-pit mining (Government of Alberta, 2017). Mining industries in Alberta, Canada affect the environment and ecosystems in various ways, such as degrading air, land, and water quality, so that reclaiming Alberta's exhausted oil sands mines has become of utmost importance (Weinhold, 2011). According to the Alberta Wetland Classification system, a wetland is a landscape that is saturated with water long enough to promote formation of water altered soils, growth of water tolerant vegetation, and various kinds of biological activity that are adapted to wet environments (Alberta Environment and Sustainable Development, 2015). Peatlands are defined as wetlands that have accumulated over 40 cm of organic matter in the form of peat (National Wetlands Working Group. 1997); they cover a large portion of the pre-disturbance landscape in northern Alberta (Vitt et al. 1996). They are globally significant ecosystems for their roles in carbon storage (Gorham, 1991). Fens are peatlands that commonly occur in the boreal region and are categorized by seasonal connections to ground and/or surface water (Vitt 2006). Considering the loss of fens to oil sands mining, Nikanotee Fen, a constructed upland-fen peatland system, was built with a combination of salvaged and mine waste mineral layers in the Athabasca oil sands region (AOSR) (Ketcheson & Price, 2016a; Ketcheson et al., 2016b; Simhayov et al., 2017; Price et al., 2010). It is a pilot study attempting to create a self-sustaining, peat accumulating fen-upland ecosystem, designed to convey water and transport solutes from the upland to the fen (Ketcheson & Price, 2016a; Ketcheson et al., 2016b). Prior studies have shown that this fen relies on groundwater derived from the upland aquifer, which was constructed from tailings sands, to sustain water levels for essential fen peatland functions (Ketcheson et al., 2017). Tailings sands are an abundant by-product of oil sands mining that contain elevated concentrations of Na^+ leachate that may be toxic to fen vegetation (Rezanezhad et al 2012; Pouliot, Rochefort, & Graf, 2012). In the constructed fen watershed, Na^+-enriched groundwater migrates from the tailings sand upland through a petroleum coke underdrain (underneath the fen and extended ~ 100 m into the upland beneath the tailings sand), to beneath the fen (Kessel et al., 2018). Since sodium-rich leachate from tailings sand may result in fen vegetation die-off, likely to more salt-tolerant species, the influence of fen water quantity and quality must be considered (Kessel et al., 2018; Pouliot et al. 2012). The timing and magnitude of the peak concentration of Na^+ at the fen surface is therefore relevant to the success of re-constructed peatlands. Numerical models of water and solute

transport can be used to assess the function of system components and to predict the timing and nature of solute redistribution. The particular peat used at Nikanotee Fen was sufficiently decomposed so that the Na^+ transport could be modelled using a single porosity model with kinematic adsorption (Simhayov et al., 2017). The high permeability coke underdrain limits groundwater and salts from discharging to the surface at the upland-fen interface (Ketcheson et al., 2017), resulting in a more even Na^+ distribution beneath, and vertical fluxes within the fen. Evapo-concentration occurs when water is lost due to evapotranspiration, which leaves the salt in the system at increasing concentrations (Kessel et al., 2018; Simhayov et al. 2018; Ketcheson & Price, 2016a; Ketcheson et al., 2016b), thus negatively affecting vegetation with low salt tolerance. During rain events, precipitation can temporarily dilute the salinity on the surface (Sumner & Belaineh, 2005) and generate surface runoff from hillslopes. The rainwater could also potentially drive solute out from the system by increasing surface water discharge, which is the only pathway for solute removal from Nikanotee Fen. A better understanding of the rates and processes contributing to salinization is required to better manage the water quality of future constructed landscapes. Na^+ distribution within deeper peat (50 ~ 150 cm below ground surface (bgs)) has been previously studied (Kessel et al., 2018), yet not within the rooting zone, where over 90% of root biomass was found in the top 30 cm of the fen (Messner et al., in prep). For this study, water sampling instruments were installed targeting 30 cm bgs with intake extended to 35 cm bgs. Therefore, the specific objectives of this research are to:

1. Assess the temporal variation and spatial distribution of Na^+ concentrations and electrical conductivity (EC) within the surface water and the shallow subsurface zone (here refers to the top 35 cm of peat) of the constructed fen.
2. Identify and quantify components of Na^+ mass balance in the surface water and shallow subsurface zone of the fen.
3. Comment on the hydrological processes governing the movement of salt, focusing on Na^+, occurring within surface water and the shallow subsurface zone of the fen.

1.2 Hypotheses

The hypotheses of this study include:

a) Water samples from the surface and shallow subsurface (0-35 cm bgs) in the fen peatland will show elevated sodium (Na^+) relative to concentration in the tailings sand (source of Na^+).

b) Water samples from rain (collected by rain gauge), surface water (from the peatland surface, before and after rain event), hillslope runoff (collected by runoff flumes installed on hillslopes),

discharge (from the v-notch), and groundwater (from the wells and piezometers) in the fen, based on ion concentration analysis, will show that the precipitation-driven discharge flushes surface water, and hence salt, from the fen out of the system.

1.3 Study site

Nikanotee Fen is a constructed upland-fen watershed in the AOSR (Figure 1-1), built with a combination of salvaged and mine waste mineral layers, and designed to transport water and solutes from the upland to the fen (Ketcheson & Price, 2016a; Ketcheson et al., 2016b; Simhayov et al., 2017). The upland (7.7 ha) was constructed with 2 – 3 m thick tailings sand on a 3% basal slope, with a thin layer (average 0.31 ± 0.15 m; Sutton & Price, 2020) of LFH-mineral mix reclaimed forest soil material on top. The fen (2.9 ha) was constructed (from bottom up) with an impermeable geo-synthetic clay liner (also underlays the upland), a layer of tailings sand (0.5 m thickness) underlying a layer of petroleum coke (0.5 m thickness) and topped with ~2 m thick sedge peat with remnants of *Sphagnum* moss, which originated from a moderate-rich donor fen (Daly et al., 2012). The petroleum coke extended ~ 100 m into the upland, an area which is referred as the transition zone. The fen was characterized as an extreme rich fen peatland system due to its relatively high EC, neutral pH and large quantity of base ions (Kessel, 2016). In 2018, new peat was added to the north-west corner of the fen (Figure 1-2) to raise the surface level, for experimental planting, which was not part of the sampling for the present study. Large rainfall events generate and contribute surface runoff at surrounding hillslopes to the southeast, east and west, that recharges the upland aquifer and ultimately reaches the fen via groundwater (Kessel et al., 2018; Ketcheson & Price, 2016a). The only outlet of this watershed was constructed near the north-east corner of the fen with a surface water discharge control structure (hereafter referred to as a "spill box") draining to a flume and into an outflow pond (Figure 1-2). Evapotranspiration within the fen (averaging 3.3 mm day^{-1} from 2013 to 2018), and groundwater inflow to the fen from the constructed upland (averaging ~224 mm $year^{-1}$ with respect to fen area from 2014 to 2018), were the dominant water fluxes, which generate an upward flow from the petroleum coke underdrain into the peat profile (Ketcheson et al., 2017).

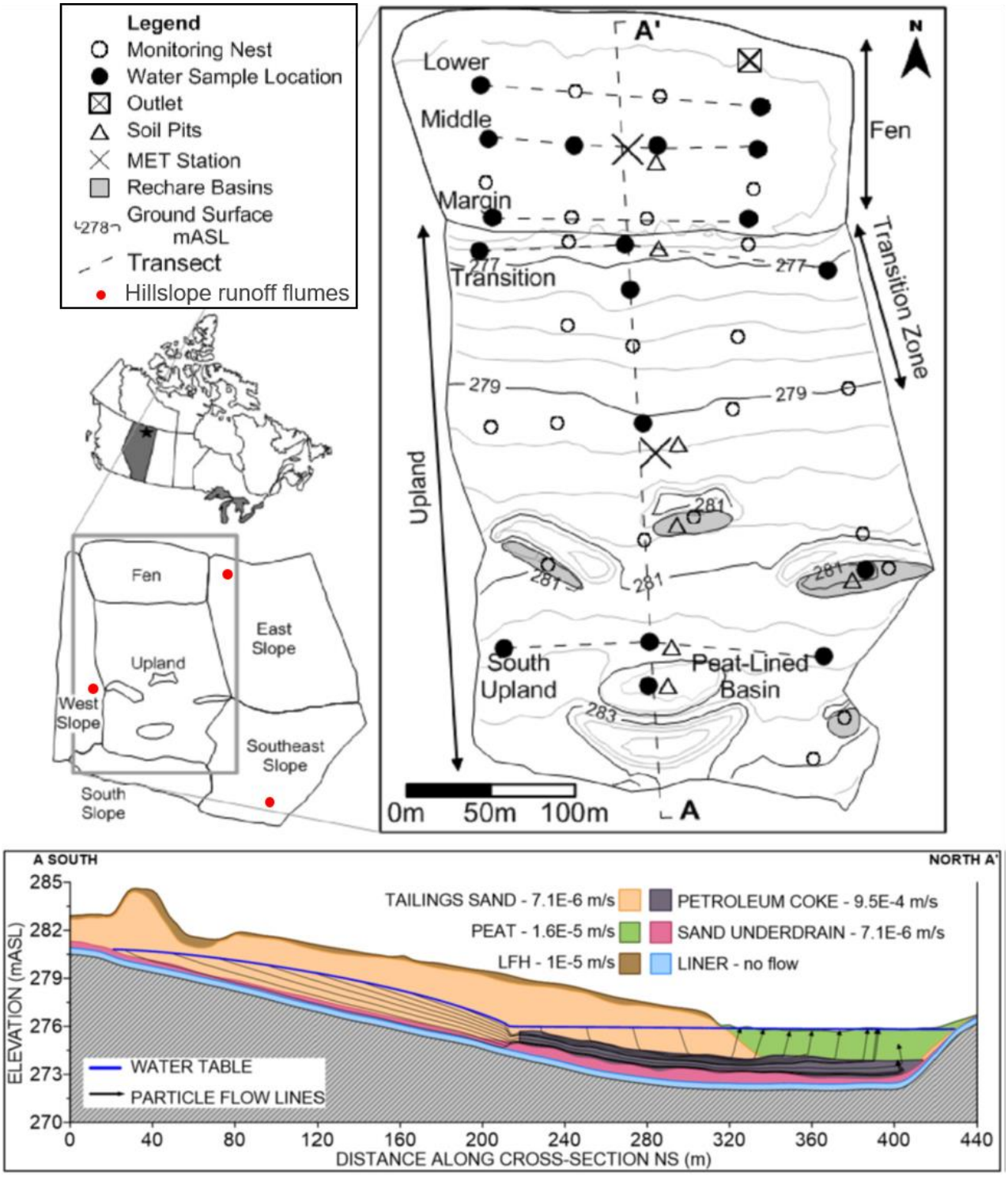

Figure 1-1 Map of Nikanotee Fen with site instrumentation and layer properties (retrieved from Kessel et al. 2018). Cross-section (bottom) illustrates the layering of materials and groundwater flow lines of particles dropped as an equal distance along the water table. The red dots showed the locations of runoff flume on each hillslope (southeast, east, and west).

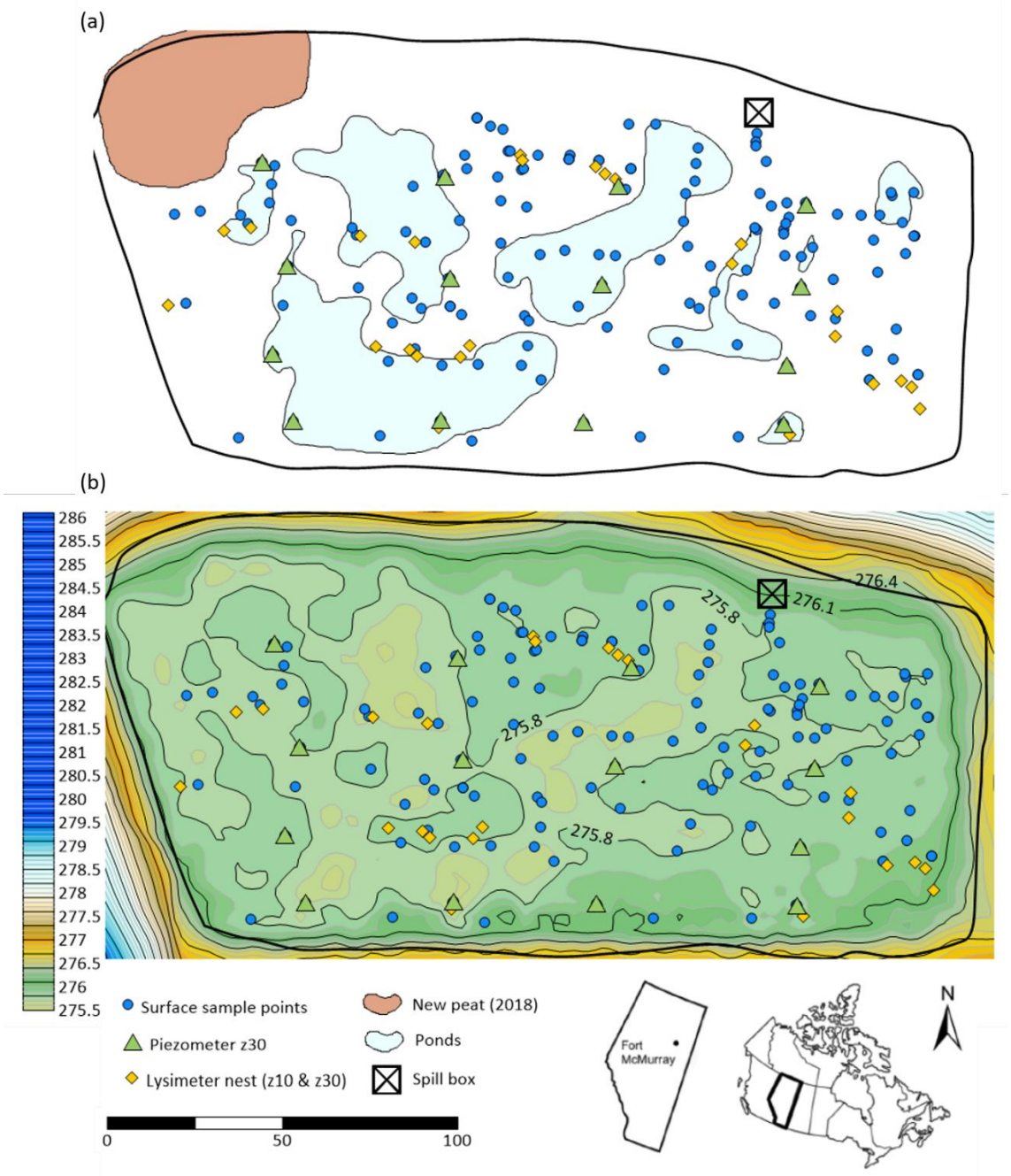

Figure 1-2 (a) Map of Nikanotee Fen with locations of sampled points (dark blue circles for ponded surface water, yellow diamonds for pore water from suction lysimeters at 10 and 30 cm bgs, green triangles for pore water from piezometers at 30 cm bgs) and ponded water (light blue shaded areas). The box with an "x" indicates the location of the spill box that redirects discharge out of the watershed. (b) Topography of the fen, collected in 2015. The observed ponded water area in 2019 matches with the areas with lower elevations in the fen.

Chapter 2
Methods

All data for this study were collected between May and August in 2019; the frost-free period (no ground ice present in the fen peat) started in early June. In this study, May is defined as a "frozen period", where fen peat was either fully or partially frozen. June 1st to late June (before the largest rainfall event on June 28th) is defined as a "dry period", with relatively low precipitation (totaling 46 mm), followed by a "wet period" occurring from June 28th to the end of August, with relatively high precipitation (totaling 217 mm).

2.1 Hydrometeorological analyses and water balance

Precipitation (*P*) was recorded cumulatively over 30-minute intervals at the upland meteorological station (Figure 1-1) using a tipping bucket rain gauge (Texas Electronic Inc TR-525M). A second tipping bucket (Onset Hobo RG3-M) located on the east slope was used to fill infrequent data gaps in recorded *P*. Actual evapotranspiration (*AET*) from the fen was estimated using the eddy covariance method at a meteorological station centered in the fen (Figure 1-1, details of the setup and procedure can be found in Ketcheson et al., 2017). Air temperature (*T*) at 2.5 m height was recorded from the meteorological station. A v-notch flume was installed upstream of the spill box to monitor surface outflow. Discharge (*Q*) was estimated using a water level pressure transducer installed at the v-notch weir, which was calibrated manually to determine a depth-discharge relationship. While *Q* through the v-notch was often zero, a loss of water from the system occurred due to lateral subsurface water seepage from the peat deposit into the spill box; a baseflow *Q* of 0.14 L s^{-1} was added to the 2019 outflow rates (Kessel et al., 2018). This amount was determined by estimating the flow in the flume below the spill box, at the entry to a storage pond. A HOBO logger was launched behind the v-notch to monitor EC every 30-minutes, which was calibrated with manual EC measurements (see 2.2.3). A monitoring network comprising nests of wells and piezometers was used to measure water levels and pressure heads across the fen (Kessel et al., 2018). There were 14 nests installed prior to this study, each with a well (150 cm total depth) and five piezometers targeting depths of 50, 90, 150, 225, 275 cm bgs, all with 20 cm slotted intake lengths. Wells and piezometers were constructed from PVC conduit (2.54 cm inner diameter (I.D.)). The water table (WT) measured by a water level logger installed at the central nest was used to represent the fen water table. Data gaps were filled using a logger in a nearby nest and calibrated by manual head measurements at each well and piezometer every other week. The nest closest to the middle of the upland near the upland meteorological station (also

the start of the transition zone) was selected for the upland water table and used with the fen water table to estimate the horizontal hydraulic gradient (Figure 1-1).

With the collected hydrometeorological data, the water balance can be calculated using the following equation (units in mm)

$$(P + GW) - (AET + Q) = \Delta S + \varepsilon \quad (1)$$

where precipitation *P* and groundwater flux *GW* were the input; actual evapotranspiration *AET* and fen runoff at the v-notch *Q* were the output; the difference between the input and the output should be equal to the change in storage ΔS with a water balance residual ε. As previously mentioned, *P* and *AET* were measured at the meteorological station with units in mm with respect to the fen area. *GW* was estimated using the following equations

$$GW = K_{sat} \cdot i_{vert} \quad (2)$$

where effective peat saturated hydraulic conductivity $K_{sat} = 65\ m\ yr^{-1}$(Kessel et al., 2018). The vertical hydraulic gradient i_{vert} was calculated using water level data between petroleum coke layer to the fen water table during the interval being examined (Eq.3).

$$i_{vert} = \frac{(h_{z225} - h_{well})}{(l_{z225} - l_{well})} \quad (3)$$

where h_{z225} & h_{well} were the head (mASL) measured in piezometer centered at 225 cm bgs with 20 cm intake, and in the adjacent well, with 150 cm intake, respectively. $(l_{z225} - l_{well})$ was the distance between water table and the mid screen of the piezometer centered at 225 cm bgs. *q* was estimated from *Q* at the v-notch with respect to the fen area. ΔS was the total of the change in storage from the beginning to the end of the studied period, calculated using the following equation

$$\Delta S = S_y \cdot \Delta WT_{bgs} + \Delta WT_{ags} \quad (4)$$

where S_y was the specific yield of the fen peat (0.05; Scarlett and Price, 2019), ΔWT_{bgs} was the water table change below ground surface, and ΔWT_{ags} was the water table change above ground surface. The error term (ε) represented the water balance residual.

2.2 Surface and groundwater sampling

To assess porewater Na^+ concentration and EC, water samples were collected from ponded surface water and pore water from the shallow subsurface zone (top 35 cm of peat) of the fen. Shallow piezometers centered at 30 cm bgs (newly installed with 10 cm slotted intake length) and suction lysimeters centered at 10 and 30 cm bgs (with 5 cm intakes) were installed to extract pore water from the shallow subsurface zone. To assess the Na^+ concentration and EC in the outflow, water samples

were collected at the outlet from the v-notch to represent surface water only samples, and below the spill box to represent mixed subsurface water samples. All samples followed the same sampling procedure in which EC and temperature were measured immediately the sample was then stored at 4 °C for the Na^+ concentrations analysis.

2.2.1 Location of surface and subsurface sampling points

The surface sampling points were selected based on the location and presence of ponded water. At the driest period, there were only 11 surface ponded water sampling points, but in the wettest conditions there were a total of 161 points. The subsurface sampling points were located near 14 pre-existing nests, with new piezometers screened at 30 cm bgs with 10 cm slotted intake length, which were installed on May 25th using the same type of PVC pipe as the pre-existing wells and piezometers (2.54 cm I.D.; Figure 1-2).

There were in total 56 EC (roughly three times per week with at least 24 hours in between) surveys over the study season, with eight of these surveys including the collection of surface and subsurface water samples for Na^+ analysis. EC was measured at every point unless it was dry, or there was no accessible water. A Thermo Scientific Orion Conductivity and Temperature probe attached to an Orion Star A325 pH/Conductivity multiparameter meter was used to measure EC and T in the field. It was calibrated to 1413 μS cm^{-1} and 12880 μS cm^{-1} standard solutions (temperature compensated to 25 °C) daily before use. The depth of the ponded surface water to the ground at each surface point was measured manually using a measuring tape. The depth to water table at each nearby well was also measured during each survey.

Approximately once every two weeks, water samples were collected from a random selection of 14 ~ 34 surface points, and all the 30 cm bgs piezometer points (Figure 2-1). They were conducted on May 29th, June 3rd, June 17th, July 1st, July 16th, July 31st, and August 13th of 2019. For surface water samples, a clean 60 ml high density polyethylene vial was used to collect samples. The vials were "environmentalized" by triple-rinsing with full volume of the sample water. The piezometers were purged (minimum 3 volumes of water in the piezometers) at least 24 hours prior to water sample collection, allowing enough time for recovery. The water samples were extracted using a Waterra^{TM} pump. To avoid cross contamination between piezometers, all devices and tubes were flushed thoroughly with de-ionized water between each sample. The water sample was taken in a clean 60 mL high density polyethylene vial and stored in a cooler at 4 °C until returned that day to the lab. Samples were stored in the fridge for 24 hours to settle the peat or sediments contained in the water samples and decanted afterwards.

Figure 2-1 Photo of a piezometer at 30 cm bgs and adjacent ponded surface water, located at the north west corner of the fen.

2.2.2 Lysimeter porewater extraction

Suction lysimeter samples (Figure 2-2; Model 1900 Soil Water Sampler, Soil Moisture Equipment Corp., Santa Barbara, California and retrofitted tensiometers) were collected at locations shown in Figure 1-2 within 24 hours of the collection of surface and piezometer samples, thus were included in this study to increase sample size and to improve spatial representation. Due to the high water-retention capacity of the peat (Scarlett & Price, 2019) it was time consuming to get a substantial volume of sample for analysis. A suction was induced using a vacuum pump to -75 kPa to all lysimeters within a 2-hour period. The following morning, water samples were collected using a 60 mL syringe connected by a three-way valve to the Tygon^{TM} tubing (sealed with black electrical tapes) of the lysimeter to extract the sample. Samples were then placed into a 120 mL sample bottle. The lysimeters were suctioned again to -75 kPa for second round of sampling conducted approximately 4 hours later the same day. Samples collected from the second round were added to the same 120 mL bottle and combined with the initial sample. EC and temperature of the sample were measured immediately after collection using the same method as for the surface and piezometer water samples. Samples were filtered using vacuum filtration through 0.45 μm nitrocellulose filters (within 24 hours of sampling).

Figure 2-2 Photo of two suction lysimeters installed at 30 cm bgs (left, with white tape) and 10 cm bgs (right, with yellow tape) in a ponded area.

2.2.3 V-notch and spill box

Water samples were collected using Teledyne ISCO 6712 full-size portable sampler at the v-notch when there was overflow, and at the spill box daily, to determine EC and Na^+ concentrations (Figure 2-3). The auto sampler was set with a trigger to be turned on when rainfall began and was set to collect 200 mL of surface outflow in 1-, 2-, or 3-hour intervals that appropriately corresponded with a rise in discharge rate. Most water samples captured discharge before or after a rain event, yet 6 (out of 72) water samples were collected during a rain event. Water samples were retrieved the next day into an “environmentalized”60 mL high density polyethylene vial.

Figure 2-3 Photos of v-notch and ISCO auto sampler. (a) an overview of the outflow setup, with ISCO auto sampler on the right. (b) a close-up view of the ISCO auto sampler collecting water from behind the v-notch. Blue arrows indicate the outflow direction.

2.2.4 Hillslopes

A runoff flume was installed at each of the surrounding hillslopes to the east (Figure 2-4), southeast, and west (areas of 8.2, 8.1, and 2.4 ha, respectively, Figure 1-1 locations shown as red dots on each slope) that collected water samples with a 60 mL high density polyethylene vial attached to the end of each flume. These flumes operated intermittently but were visually inspected daily for water samples. If there was water in the attached vial, the vial was capped and removed for analysis and replaced with a new vial for further sampling.

Figure 2-4 Runoff flume installed on the east slope. (a) one end of the flume was instrumented with sample bottle attached to collect runoff water sample. A pressure transducer installed in the bucket was used to estimate flow. (b) flow-collector above the flume, sealed with hydraulic cement.

2.3 Na^+ concentrations and validation

Between 3 to 10 mL of water sample volume was used to measure Na^+ concentrations using an Orion Star A324pH/ISE multiparameter meter with a ROSS Sodium Sure Flow Electrode (model 8611BNWP). The probe was calibrated before use and after every 2 hours of use with 10, 100, and 1000 ppm standards. After each calibration, the electrode slope was obtained and checked according to the manual to ensure proper function. To prepare the sample, the water was mixed with Ionic Strength Adjuster (ISA) at a ratio of 10:1 (each 10 mL of sample was mixed with 1mL of ISA), which was used

to keep a near-constant background ionic strength and to adjust the pH. The probe was put into the stirred mixture to measure the concentrations, then the mixture was disposed afterwards.

To validate the Na^+ concentrations measured by the probe, a total of 100 randomly selected samples from surface, piezometer, v-notch and spill box water locations were analyzed by a Dionex ICS-1600 Method EPA 300.0 with AS-DV auto-sampler with analytical precision to ± 1.0 mg L^{-1}. These samples were filtered using syringe filtration through 0.45 μm nitrocellulose filters, then 1:10 diluted with ultrapure deionized water. The Na^+ concentrations measured by the Dionex were then compared with the Na^+ concentrations measured by probe for validation. The fitting curves are shown in Appendix A. The relationship was found to be $C_{Dionex} = 1.2 \times C_{Orion}$ ($R^2 = 0.97$), which was used to adjust all probe-measured Na^+ concentrations for this study.

2.4 Statistical analyses

The Kruskal-Wallis test is a non-parametric test that assesses whether statistically significant differences exists between multiple groups of variables using the relative rankings within the different samples (Kruskal & Wallis, 1952). The Wilcoxon rank sum test is a non-parametric test used for pairwise comparisons (Wilcoxon, 1945). These analyses were performed using R, a language for statistical computing (R Core Team, 2013), to determine if dependent variables Na^+ concentration (or EC) from multiple categories, including spatial (surface (surf), 10 cm bgs (z10), and 30 cm bgs (z30)) and temporal (dry period and wet period), respectively, are identical or if at least one of the categories tends to give observations that are different from those of other categories ($\alpha = 0.05$).

2.5 Surfer interpolation

Na^+ concentrations and EC spatial distribution in plan-view (x-axis versus y-axis) were contoured using a 2D contour kriging interpolation package in Surfer® 17 (Golden Software, LLC), presented in three separate layers of the fen: surface water, 10 and 30 cm bgs. The water table height relative to ground surface, using data from surface ponded water depth and water table measured in wells, were also contoured using the kriging interpolation package on each sampling date. The grid nodes for contour interpolation, whose values were based on the known data points neighboring the node. The known data points are sampled points plotted using its x- and y-value coordinates, with the corresponding Na^+ concentrations, EC, or water table heights as z-value. Each data point is weighted by its distance from the node, using the following equation (Golden Software, 2020):

$$Z_A = \sum_{i=1}^{n} W_i Z_i \quad (5)$$

where Z_A is the estimated value of grid node A, n is the number of neighboring data values used in the estimation, Z_i is the value at location i with weight, W_i. The value of weights will sum to 1 to make sure there is no bias towards clustered data points (Golden Software, 2020). The default ordinary kriging was used for this study. It is acknowledged that kriging is an interpolation tool and that regions between observation points do not reflect the actual in-situ concentrations.

2.6 Mass balance

To minimize the influence from snow water recharge on Na^+ concentrations, only the samples collected in the frost-free period from June 3rd to August 13th, 2019 (total of 72 days) were used to estimate Na^+ mass balance in the top 35 cm of the fen. The Na^+ mass balance was estimated using:

$$\Delta Na_{Tot} + \varepsilon = (GW \cdot C_{GW} + P \cdot C_P + R \cdot C_R) - (Q \cdot C_Q + AET \cdot C_{AET}) \quad (6)$$

where, the left side of the equation includes the change in Na^+ mass measured in ponded surface water and subsurface peat (ΔNa_{Tot}, between June 3rd and August 13th) and an error term (ε), whereas the right side of the equation is used to estimate Na^+ mass in the hydrological fluxes, where C is concentration, GW, P, R, Q and AET are groundwater inflow, precipitation, runoff from hillslopes, discharge at the v-notch weir and actual evapotranspiration, respectively, for the mass budget period. The results from both side of the equation will be compared and discussed.

2.6.1 Na^+ mass measured in ponded surface water and subsurface peat

The left side of Eq.6 is the estimated change in total Na^+ mass contained in the ponded surface water and in the top 35 cm of peat (Na_{Tot}, kg), thus, it contains three elements: Na^+ in ponded surface water (Na_{water}, kg, Eq.7); Na^+ in unsaturated peat (Na_{unsat}, kg, Eq.8); and Na^+ in saturated peat (Na_{sat}, kg, Eq.9). The fen was partitioned into an array of cells and each contained one 30 cm depth piezometer (z30, green triangles, Figure 2-5 (a) & (b)); a variable number of suctions lysimeters at 10 and 30 cm bgs (depending on whether the suction lysimeter was allocated to the saturated or unsaturated zone on a given date) to sample porewater (z10 and z30, yellow diamonds, respectively, Figure 2-5 (a)); and a variable number (depending on the extend of ponding on the given date) of ponded surface water samples (surf, dark blue circles, Figure 2-5 (a)). All points shown on Figure 2-5 had EC and water depth measurement, but only selective ones had Na^+ concentration measured. There were in total 8 Na^+ sampling events in the field (May 29th, June 3rd, June 17th, July 1st, July 16th, July 26th, July 31st and August 13th, 2019), but only 6 (excluding May 29th since it was in the frozen period, and July 26th due to missing surf samples) were used for the mass balance. The total sample size (including surf, z10 and z30) increased from 80 (June 3rd) to 101 (August 13th) as the fen became wetter.

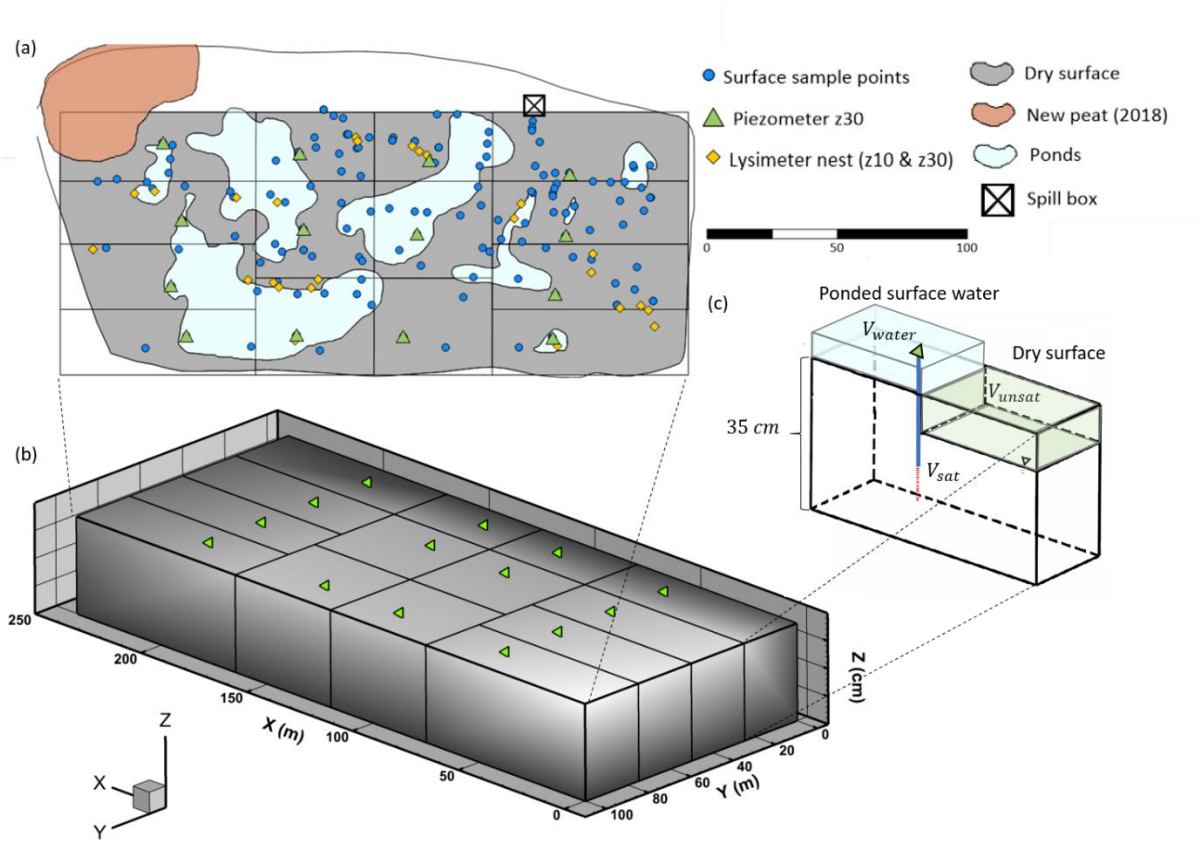

Figure 2-5 Simplified fen cells for sodium mass storage estimation. 14 cells were used in this model, with conceptual water table to demonstrate unsaturated and saturated zones of peat. (a) the plan view of the conceptual model with sample point locations in the fen. (b) the 3-D view of the conceptual model of 0 ~ 35 cm of peat. (c) a simplified example of a single fen cell with half dry surface with unsaturated peat, and half ponded surface water on top of the peat containing one piezometer at 30 cm bgs.

The water table height relative to ground surface (z-value) contours were created using kriging in Surfer, where positive z means cm of water above ground surface, and negative z means cm of water below ground surface, with the coordinates as x- and y-values (Figure 3-6). The Grid Volume command calculated cut (positive) and fill (negative) volumes ($x \cdot y \cdot z$) between the upper surface and the lower surface, within each cell. The positive portion is the volume between the upper and lower surface when the upper surface is above the lower surface; whereas the negative portion is the volume between the upper and lower surfaces when the upper surface is below the lower surface (Golden Software, 2019). In this case the upper surface is the water table contours on each individual sampling date and the lower surface is the ground surface (z = 0) or the bottom boundary (z = -35). With the ground surface set as a constant z = 0, the positive volume above z is the ponded surface water volume (V_{water}, m^3), and the negative volume below z is the unsaturated peat volume (V_{unsat}, m^3; Figure 2-6, top figure). When the lower surface is set as z = -35, the positive volume above z is the ponded surface water plus saturated

peat volume (V_{-35}, m^3; Figure 2-6, bottom figure). To get the saturated peat volume (V_{sat}, m^3), the ponded surface water volume (V_{water}) is subtracted from the total volume (V_{-35}) so that $V_{sat} = V_{-35} - V_{water}$.

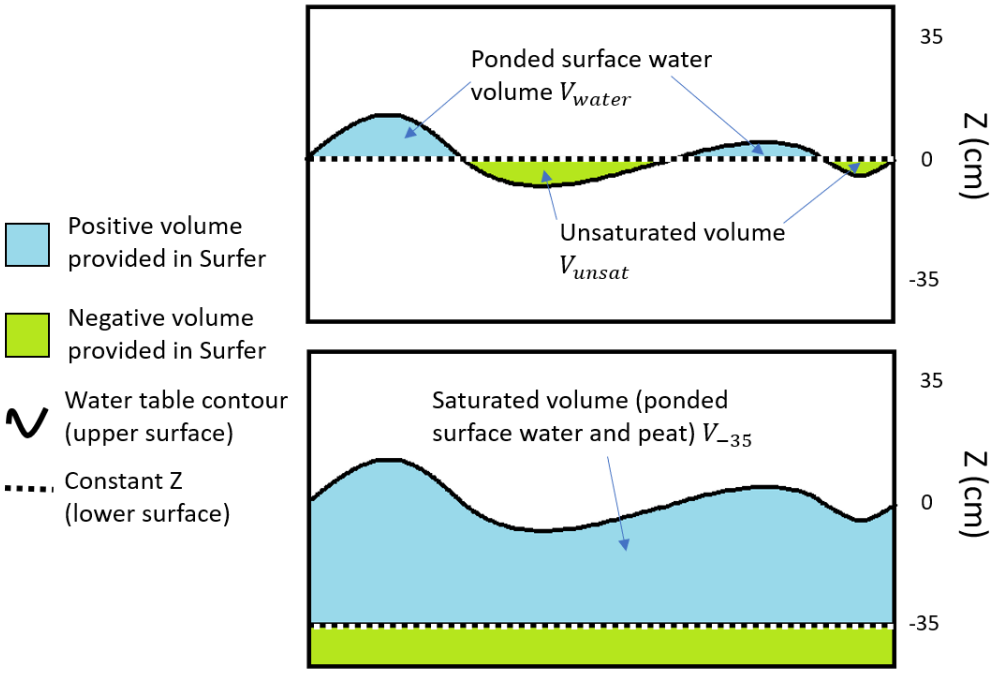

Figure 2-6 Conceptual cross-section diagram of volumes calculated using Grid Volume command (not to scale). The top figure is when lower surface is set as a constant z = 0 and the bottom figure is when lower surface is set as the bottom boundary of this study (top 35 cm peat, when z = -35).

For Na_{water} in each cell on each date,

$$Na_{water} = V_{water} \cdot C_{water} \quad (7)$$

where C_{water} (kg m^{-3}) is average Na^+ concentration of surf samples for that date. For cells that did not contain any Na^+ sampled points, since all surf points had EC measurement, Na^+ concentrations were estimated from EC with $C_{Na} = 0.1399 \times EC - 92.734$ ($R^2 = 0.79$). This equation was the best-fit-line of EC and Na^+ concentration in all surf samples (Figure B. 1).

For Na_{unsat} in each cell on each date,

$$Na_{unsat} = V_{unsat} \cdot C_{unsat} \cdot \theta \quad (8)$$

where C_{unsat} (kg m^{-3}) is average Na^+ concentration of points z10. For cells that that did not contain any sampled points (red shaded cells, Figure B. 2), daily averaged C_{unsat} of its adjacent cells (Table B. 2) was used to fill the gap. θ is the average of volumetric water content measured hourly during the study

period using soil moisture probes (Stevens Hydra II probes) connected to Campbell Scientific CR 1000 dataloggers at depth from 0 to 30 cm bgs (Ketcheson et al., 2017).

For Na_{sat} in each cell on each date,

$$Na_{sat} = V_{sat} \cdot C_{sat} \cdot \theta \quad (9)$$

where C_{sat} (kg m^{-3}) is average Na^+ concentration of points z30 (including lysimeters and piezometers) and points z10 when they were below water table. θ is the average of volumetric water content of the peat, which being saturated was assumed to equal the porosity of the peat.

Therefore, the sum of these three elements Na_{water}, Na_{unsat} and Na_{sat} of all cells on each date will yield Na_{Tot} on each date:

$$Na_{Tot} = Na_{water} + Na_{unsat} + Na_{sat} \quad (10)$$

Then Na_{Tot} from August 13th minus Na_{Tot} from June 3rd is the change in seasonal Na^+ mass measured in ponded surface water and subsurface peat (ΔNa_{Tot}). The error term (ε) was determined as a residual once the Na^+ mass in fluxes (right side of Eq.6) were estimated.

2.6.2 Na^+ mass in fluxes

The right side of Eq.6 indicated Na^+ mass in the hydrological fluxes, where C (mg L^{-1}) is Na^+ concentration within each flux. The sodium mass input is calculated using the sum of sodium mass contained in 1) groundwater recharge from upland tailings sand through the petroleum coke underdrain towards peat, $GW \cdot C_{GW}$; 2) precipitation, $P \cdot C_P$; and 3) surface runoff from hillslopes to fen, $R \cdot C_R$; whereas the sodium mass output was calculated by the total of sodium mass lost in discharge, $Q \cdot C_Q$, and evapotranspiration, $AET \cdot C_{AET}$ (Figure 2-7). Since C_{AET} is essentially zero, Na^+ mass from evapotranspiration is assumed to be zero. From 2013 to 2016, average C_P was 8.6 mg L^{-1} (unpublished), which was two orders of magnitude less than C_{GW}, thus, C_P is assumed to be negligible. Similarly, $R \cdot C_R$ is assumed to be negligible, because from the southeast, east, and west slopes, the total depth of R with respect to each slope area over the study period (May 18th to August 31st) was 0.2, 0.2, and 3.8 mm, respectively; and C_R were 24.7, 7.4, and 9.6 mg L^{-1}, respectively, which was almost two orders of magnitude less than GW and C_{GW}. Groundwater recharge and stream discharge, therefore, are the dominant components to assess the mass balance input and output, respectively.

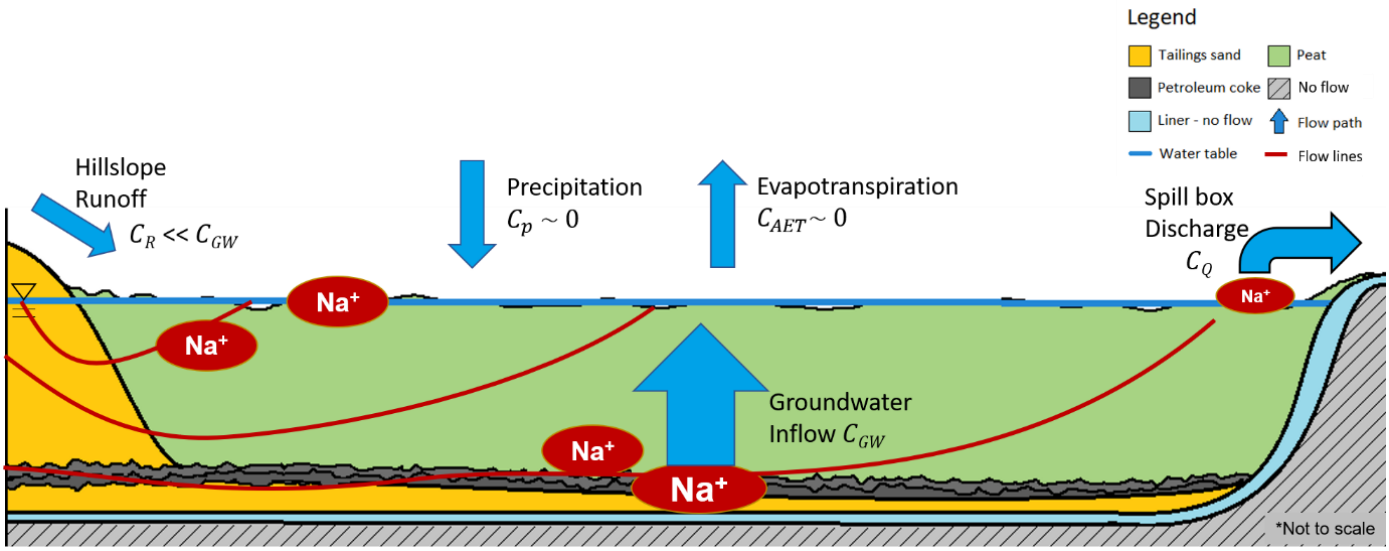

Figure 2-7 Conceptual salt budget model (not to scale), demonstrating flow lines (red lines) and potential pathways for Na^+ movement (blue arrows).

For each cell on each period interval (Appendix H), groundwater inflow of Na^+ to the fen, M_{GW} (kg day^{-1}), was estimated using the following equation:

$$M_{GW} = GW \cdot C_{GW} \cdot A \quad (11)$$

where the groundwater flux GW was estimated using Eq.2. The Na^+ concentration in groundwater, C_{GW}, was the average of Na^+ concentration measured from the piezometers centered at 30 and 50 cm bgs, incorporated with lysimeters centered at 30 cm bgs when available. The area, A, varies for each cell, with a total of 2.3 ha. Once M_{GW} for each cell within each interval was calculated, the total of the 14 cells was the total Na^+ mass estimated in the groundwater flux within each interval. Then, the total of 5 intervals was the Na^+ mass in groundwater flux for the entire studied period. Limitations of this method are discussed in Appendix H.

Discharge output of Na^+, M_Q (kg day^{-1}), was estimated using Eq.12, where Q is daily discharge (L day^{-1}), and C_Q (kg L^{-1}) is daily average Na^+ concentrations found in discharge.

$$M_Q = Q \cdot C_Q \quad (12)$$

C_Q was estimated from calibrated EC collected in 30-minute intervals from July 2nd to September 24th, 2019. More details of calibration and validation processes are in Appendix C. The average of all measured Na^+ concentrations at the outlet, 240 mg L^{-1}, was used for missing daily values.

Chapter 3

Results

3.1 Hydrometeorology

The hydrological context is reported from May 18th to August 31st (day of year (DOY) 138 to 243, duration of 106 days) for overall 2019 study season hydrometeorology, and from Jun 3rd to August 13th (duration of 72 days) for the water balance calculation in Table 3-1. In 1981 – 2018, long-term mean air temperature and total P were 15.4 °C and 224 mm for the same period (from May 18th to August 31st), respectively (Government of Canada, 2020). Thus, 2019 study season was a relatively wet and cool season compared to the climate normals.

Table 3-1 Hydrological and water balance components for 2019, including precipitation P, actual evapotranspiration AET (potential evapotranspiration PET), fen runoff q, groundwater flux GW, change in storage ΔS, water balance residual ε, and average air temperature T. Units in mm unless specified.

Study period [a] days	P	AET (PET)	q[b]	GW[c]	ΔS[d]	ε	T °C
106	264	272 (361)	61	26	60	-103	14.0
72	182	194 (253)	44	17	41	-79	14.2

[a] Values for study period (106 days, from May 18th to August 31st) were expressed with respect to the fen area (2.9 ha) for overall 2019 study season hydrometeorology. Values for frost-free period (72 days, from June 3rd to August 13th) were expressed with respect to the mass balance total cell area (2.3 ha) for mass balance calculation.
[b] Fen runoff q was estimated using $q = Q/A$, with a seasonal average of 0.6 mm day^{-1}.
[c] Groundwater flux was estimated using Eq.2, with a seasonal average of 0.24 mm day^{-1}.
[d] Change in storage was estimated using Eq.4, with a seasonal average of 0.57 mm day^{-1}.

The Nikanotee Fen Watershed received frequent but small P events, however, the growing season was punctuated by 6 relatively intense and high-magnitude events (>10 mm day^{-1}, Figure 3-1) in 2019. May and early June (1st – 27th) was a relatively dry period (fewer and less-intense events, totaling 46 mm) comparing to the rest of the year. June 28th to the end of August was a relatively wet period (more frequent and intense events, totaling 217 mm). The fen AET rates ranged from 0.5 to 4.4 mm day^{-1} with an average of 2.6 mm day^{-1} over the 2019 season, with higher values in June and July (Figure 3-2). Cumulative $P - AET$ (Figure 3-2) had a similar trend to water table (Figure 3-1), both decreasing in the dry period. Discharge Q was low in the dry period but started to increase as it responded to P early in the wet period (<1 day, Figure 3-1). The peak q (1.9 mm, with Q = 0.62 L s^{-1})

with respect to the fen area (2.9 ha) occurred near the end of the season (August 17th), aligning with the largest *P* event (38 mm) on August 16th.

The groundwater flow direction was consistently from upland to fen. The average horizontal hydraulic gradient from the center of the upland (also the beginning of the transition zone) to the center of the fen and was 0.0024 (2019), similar to values reported in previous years (average of ~ 0.0027 between 2014 and 2016; Kessel et al., 2018). Within the 14 fen cells, the vertical hydraulic gradient between petroleum coke and water table was ranged from –0.083 to 0.056 (average of-0.00087 ± 0.02 standard deviation, with an average of -0.0097 in the dry period and an average of 0.0029 in the wet period, where a negative value means water flowing in a downward direction, from water table to petroleum coke and a positive value means in an upward direction from petroleum coke to water table, Figure I. 1). The water table within the fen was ~9 to 16 cm bgs during the frozen and dry period (Figure 3-1). It increased rapidly in response to *P* events, then remained near the surface in the wet period (~ 1.5 cm above ground surface (ags) to 11 cm bgs).

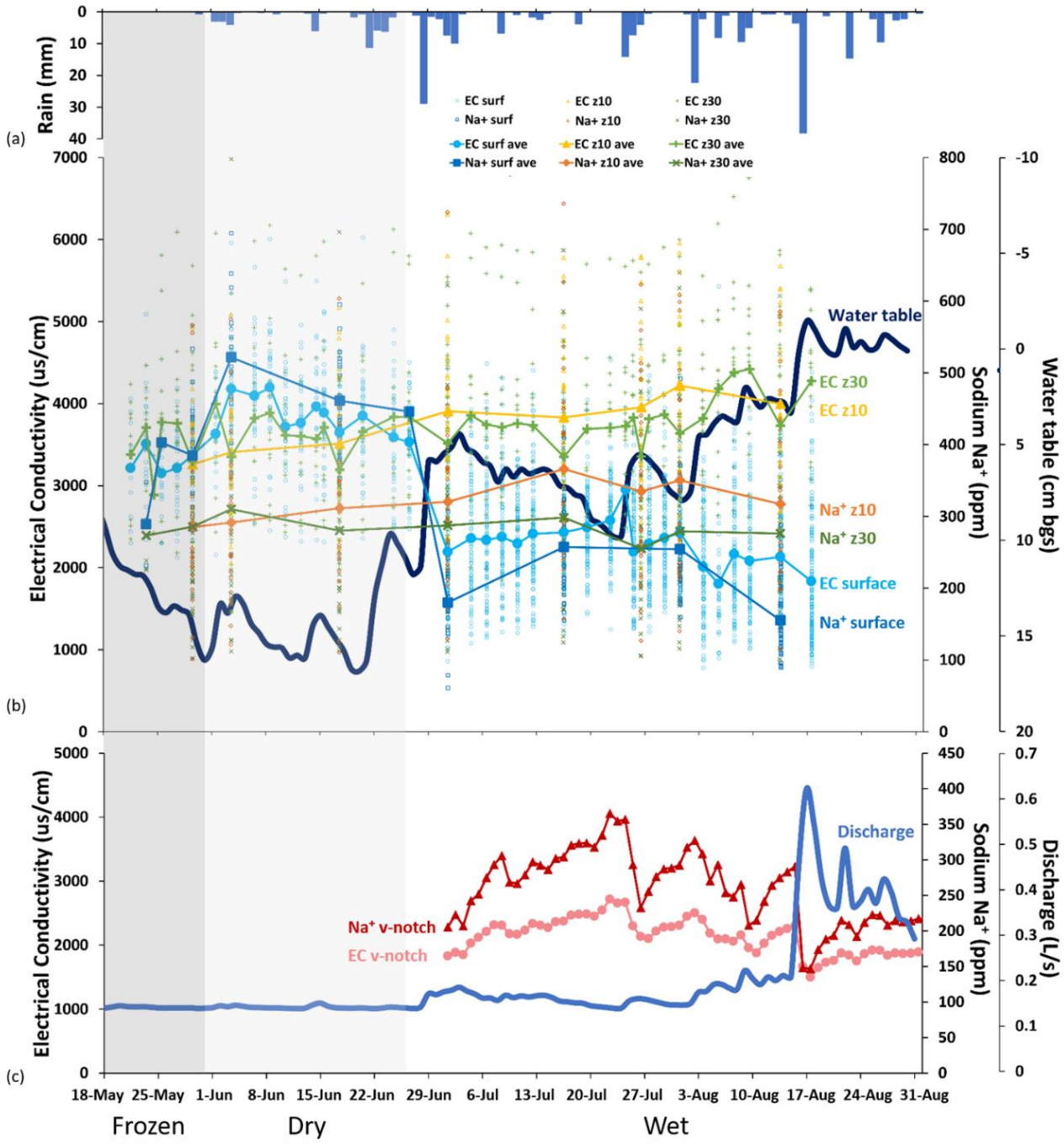

Figure 3-1 Summary of field data collected between May 18th and August 31st, 2019 including: (a) *P*; (b) water table, Na^+ concentrations and EC measured from ponded surface water, 10 and 30 cm bgs, and their daily averages; and (c) discharge, Na^+ concentrations and EC in discharge (Na^+ concentrations estimated and validated with calibrated EC measured by HOBO). Here, frozen period contains data collected in May, the dry period starts from June 1st to just before the largest rainfall event on June 28th, and the wet period includes data collected from June 28th to the end of August.

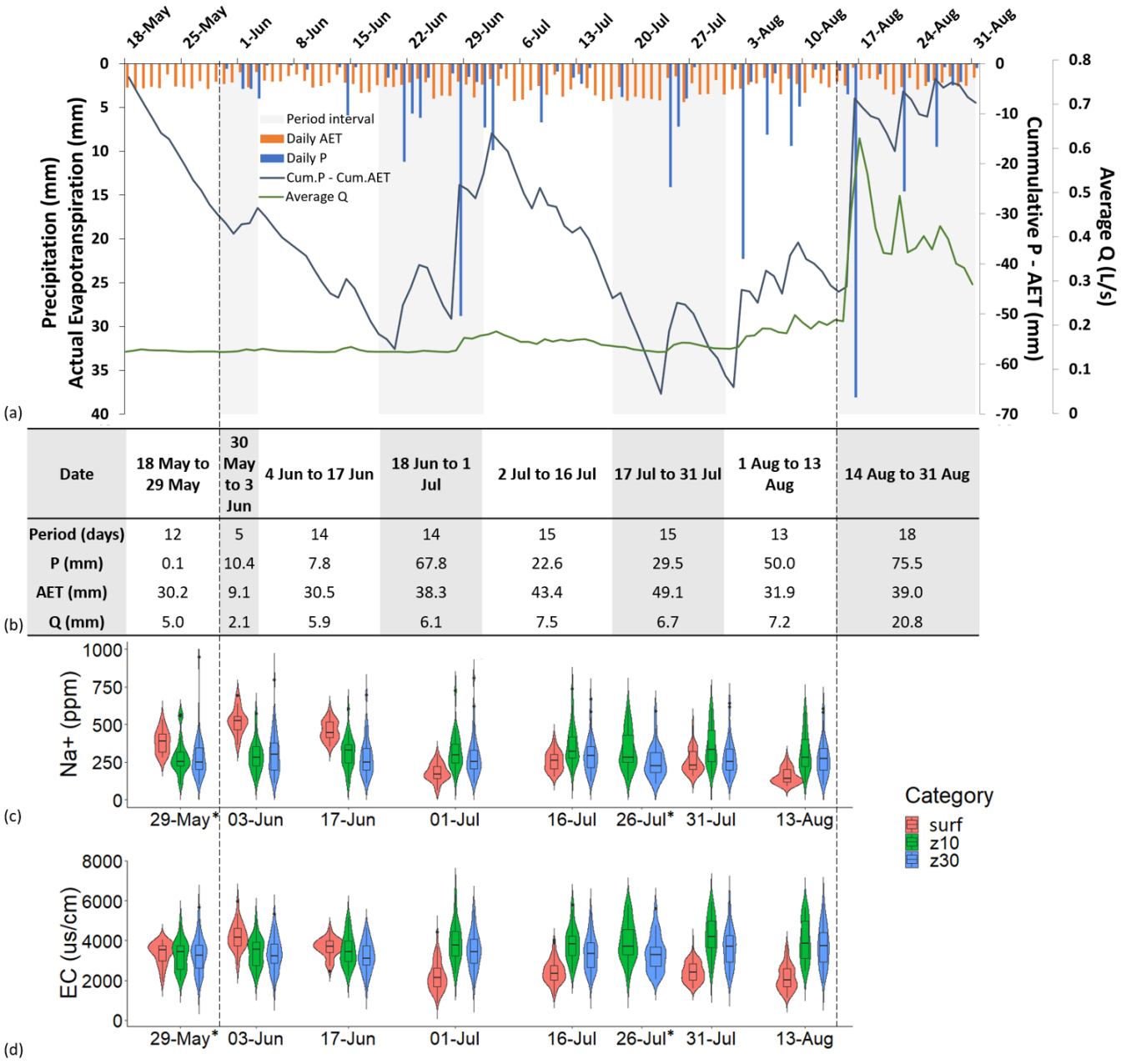

(b)

Date	18 May to 29 May	30 May to 3 Jun	4 Jun to 17 Jun	18 Jun to 1 Jul	2 Jul to 16 Jul	17 Jul to 31 Jul	1 Aug to 13 Aug	14 Aug to 31 Aug
Period (days)	12	5	14	14	15	15	13	18
P (mm)	0.1	10.4	7.8	67.8	22.6	29.5	50.0	75.5
AET (mm)	30.2	9.1	30.5	38.3	43.4	49.1	31.9	39.0
Q (mm)	5.0	2.1	5.9	6.1	7.5	6.7	7.2	20.8

Figure 3-2 (a) bar plot of *P* and *AET* with cumulative *P* – *AET* line and discharge line; (b) summary table of *P*, *AET*, and *Q* (with respect to the fen area, 2.9 ha) within every sample events intervals (grey shaded); (c) violin plots of Na^+ concentrations within ponded surface water (surf), 10 cm bgs (z10) and 30 cm bgs (z30) from each sample events; (d) violin plots for EC within surf, z10 and z30 from each sample events. A violin plot is hybrid of a box plot in the center, which shows the median, interquartile range (first and third quartile), lower/upper adjacent values, and outliers; and a kernel density estimate, which is a non-parametric depiction of the probability density function (Hintze & Nelson, 1998). *samples collected on these dates were excluded for mass balance calculation.

3.2 Na^+ concentrations and EC distribution

Generally, average Na^+ concentrations and EC found in the shallow subsurface peat were the highest and gradually decreasing within deeper peat, whereas values at the surface were smaller and more variable comparing to 10 cm bgs. (Figure 3-3). Seasonal Na^+ concentrations and EC found in the ponded surface water and shallow subsurface peat of the fen were 292 ± 129 mg L^{-1} and 2885 ± 1032 µs cm^{-1}, respectively (Table 3-2). Na^+ concentrations and EC were not normally distributed (Figure 3-2 (c) & (d)). For the three water sampling events in May and June, Na^+ concentrations and EC within ponded surface water were generally higher than at 10 and 30 cm bgs, with a smaller range. In contrast, Na^+ concentrations and EC in July and August were generally lower for ponded surface water relative to 10 and 30 cm bgs (Figure 3-2, Figure 3-3, Table 3-3).

The Kruskal-Wallis test showed that seasonal Na^+ concentrations were significantly different between ponded surface water and 10 cm bgs, and between 10 and 30 cm bgs, whereas it was not significantly different between ponded surface water and 30 cm bgs (Figure 3-4). Yet, seasonal EC was significantly different between all three categories. For ponded surface water samples, Na^+ concentrations were significantly different between the dry and wet period (Figure 3-5), however, for water samples within 10 and 30 cm bgs, Na^+ concentrations were not significantly different between dry and wet periods. On the contrary, for all three categories, EC was significantly different between the dry and wet period.

Na^+ concentrations and EC were generally higher during the dry period and lower during the wet period (Figure 3-2 (c) & (d), Table 3-2). A *P* event on June 28th (29 mm), increased water tables and decreased average Na^+ concentrations and EC of ponded surface water, however, samples collected from 10 and 30 cm bgs did not vary substantially (Figure 3-2 (c) & (d), between June 17th to July 1st). Average Na^+ concentrations and EC of ponded surface water was highest during the dry period, then decreased following multiple *P* events in late June by 61% (from 462 to 181 mg L^{-1}) and 40% (from 3652 to 2199 µS cm^{-1}), respectively (Figure 3-1, Figure 3-2, Appendix G). In contrast, average Na^+ concentrations at 10 and 30 cm bgs remained steady from the dry period to the wet period (statistically non-significant shown in Figure 3-5 (a)). Unlike Na^+ concentrations, average EC at 10 and 30 cm bgs increased slightly from the dry period to the wet period (Figure 3-5 (b)). Over the duration of the study, the pH of fen peat was generally neutral (mean pH of 7 ± 0.17).

Table 3-2 Mean Na^+ concentrations and EC (± Standard Deviation) within ponded surface water and subsurface peat, from frozen, dry, and wet period. Bolded values denote the highest average of all periods.

Period	Frozen	Dry	Wet	Average
Na^+ (mg L^{-1})	304 ± 129	**341 ± 138**	272 ± 121	292 ± 129
EC (µS cm^{-1})	3379 ± 726	**3721 ± 743**	2601 ± 978	2885 ± 1032

Table 3-3 Seasonal mean Na^+ concentrations and EC (± Standard Deviation) within peat, from ponded surface water (surf), 10 cm bg (z10), 30 cm bgs (z30), 50 cm bgs (z50) surface discharge at v-notch (ISCO), and discharge at spill box (SB). Sample numbers ranged from 11 to 2396 for each category.

Category	surf	z10	z30	z50*	ISCO**	SB**
Na^+ (mg L^{-1})	291 ± 143	324 ± 123	286 ± 128	236 ± 148	228 ± 66	220 ± 68
EC (µs cm^{-1})	2587 ± 903	3777 ± 942	3666 ± 942	3641 ± 926	1957 ± 310	2796 ± 556

* 10 groundwater samples taken each month (June, July, and August) from piezometers in the fen peat at 50 cm bgs with 20 cm slotted intake length (sample size n = 30).
** Manual measurement at outflow used for calibration and validation of Na^+ concentrations and EC measured by HOBO, therefore not shown in Figure 3-1and Figure 3-2.

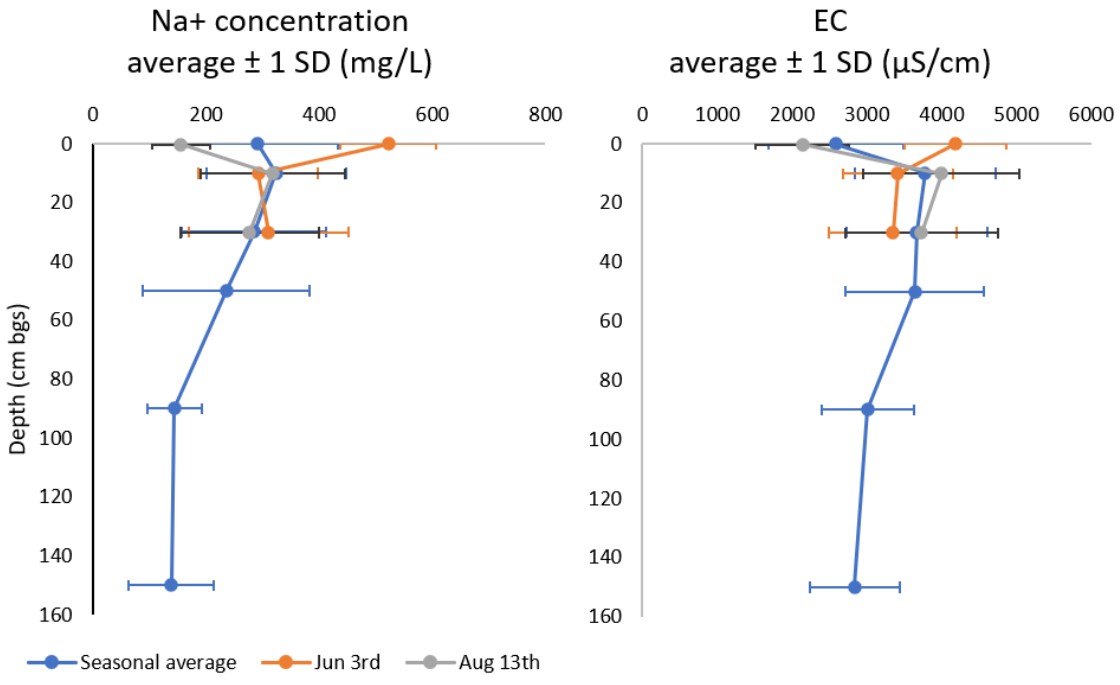

Figure 3-3 Average ± 1 Standard Deviation of Na^+ concentration and EC by depth below ground surface in fen peat.

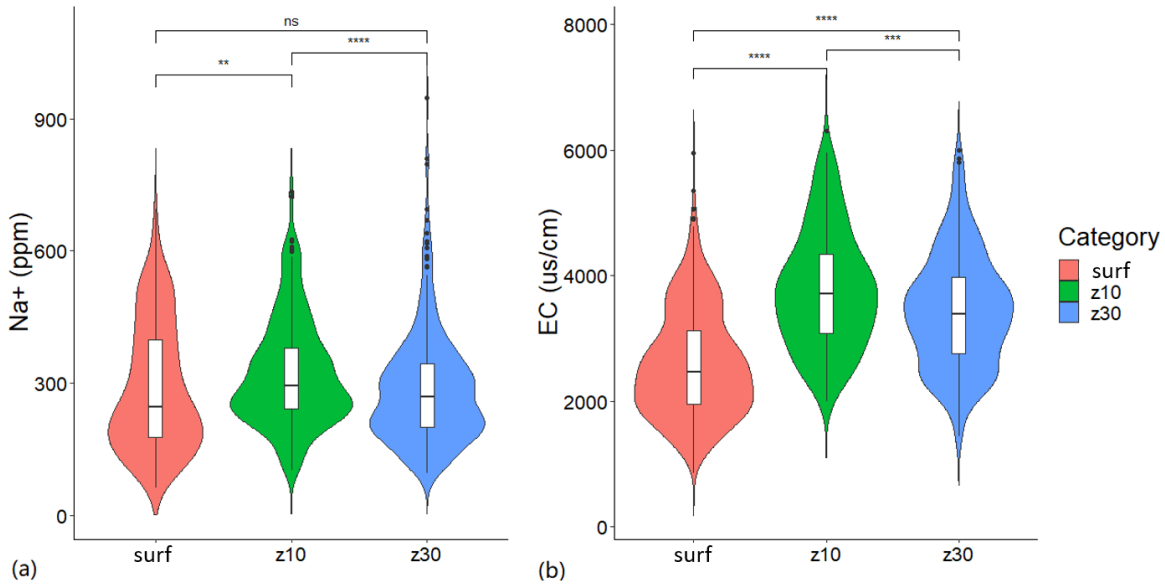

Figure 3-4 Seasonal Na^+ (a) and EC (b) measured from ponded surface water (surf), 10 cm bgs (z10) and 30 cm bgs (z30) using Wilcoxon rank sum test ($\alpha = 0.05$) for pairwise comparisons. Note that ns means not significant at any level equal to 0.05 or higher, whereas *, **, * and **** indicate significance at p<0.05, 0.01, 0.001 and 0.0001, respectively.**

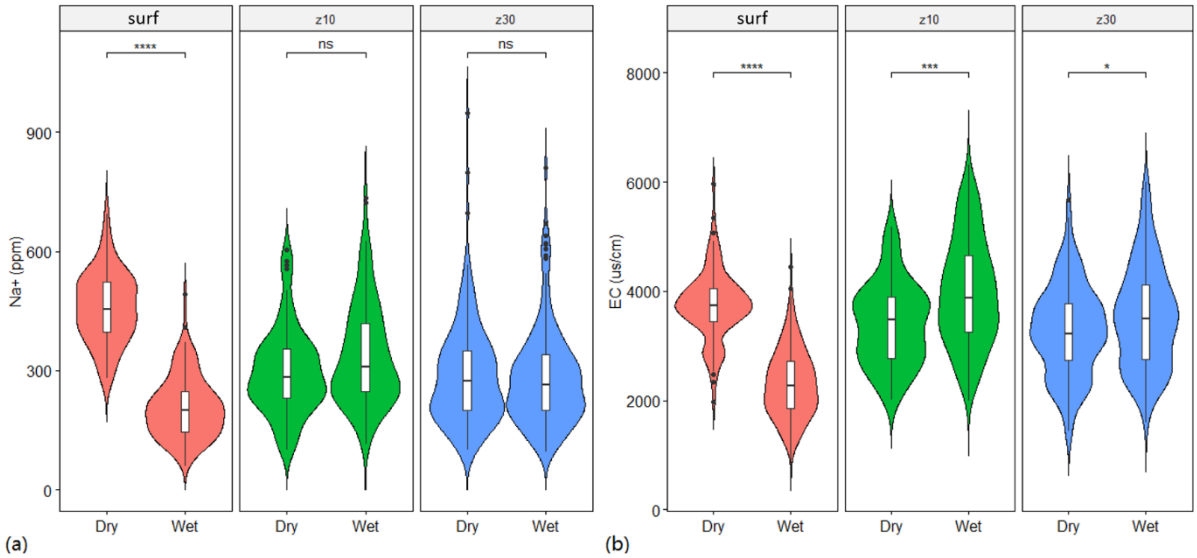

Figure 3-5 Na^+ (a) and EC (b) by category including ponded surface water (surf), 10 cm bgs (z10) and 30 cm bgs (z30) and tested difference between dry and wet periods as previously defined. Note that ns indicates not significant, whereas *, **, *, and **** indicate significance at 0.05, 0.01, 0.001 and 0.0001, respectively.**

3.3 Spatial interpolation and temporal patterns

Average water table depths in the dry period and wet period are illustrated in Figure 3-6. The plan-view interpolation maps show the spatial and temporal patterns of 2019 Na^+ concentrations (Figure 3-7 ~ Figure 3-9) and EC (Figure 3-10 ~ Figure 3-12) in the fen peatland, within ponded surface water, 10 and 30 cm bgs in 2019. The kriged contours show that in ponded surface water, 10 and 30 cm bgs, Na^+ concentrations and EC were generally the highest at the south-west corner, where it was consistently the wettest part of the fen with average water table 16 cm ags; and lowest at the north and east portion of the fen, where it was relatively dry (average water table 1.5 cm bgs, Figure 3-6). A pathway of elevated Na^+ appeared in the central part of the fen within ponded surface water and 10 cm bgs, trending towards the spill box (Figure 3-7 & Figure 3-8). Similar patterns were found for EC in ponded surface water, except that on June 3rd, the highest EC occurred at the east part of the fen (Figure 3-10). Lower EC in ponded surface water was normally found at locations of persistently ponded water. Temporal patterns in ponded surface water show that Na^+ concentrations and EC were higher in the early season (dry period) with low *P*, high *AET*, and lower water table (Figure 3-7 & Figure 3-10). Na^+ concentrations and EC decreased immediately following the substantial rainfall received in late June and August. Higher concentrations are consistent with lower precipitation and enhanced drying. Conversely, Na^+ concentrations and EC at 10 and 30 cm bgs remained relatively consistent over time, with a slight increase in the wet period and remained consistent thereafter (Figure 3-8, Figure 3-9, Figure 3-11, & Figure 3-12). They were less sensitive to precipitation and were steadier comparatively over time. Similarly, the hotspot in the south-west corner and lower values near the discharge were also observed at 10 and 30 cm bgs.

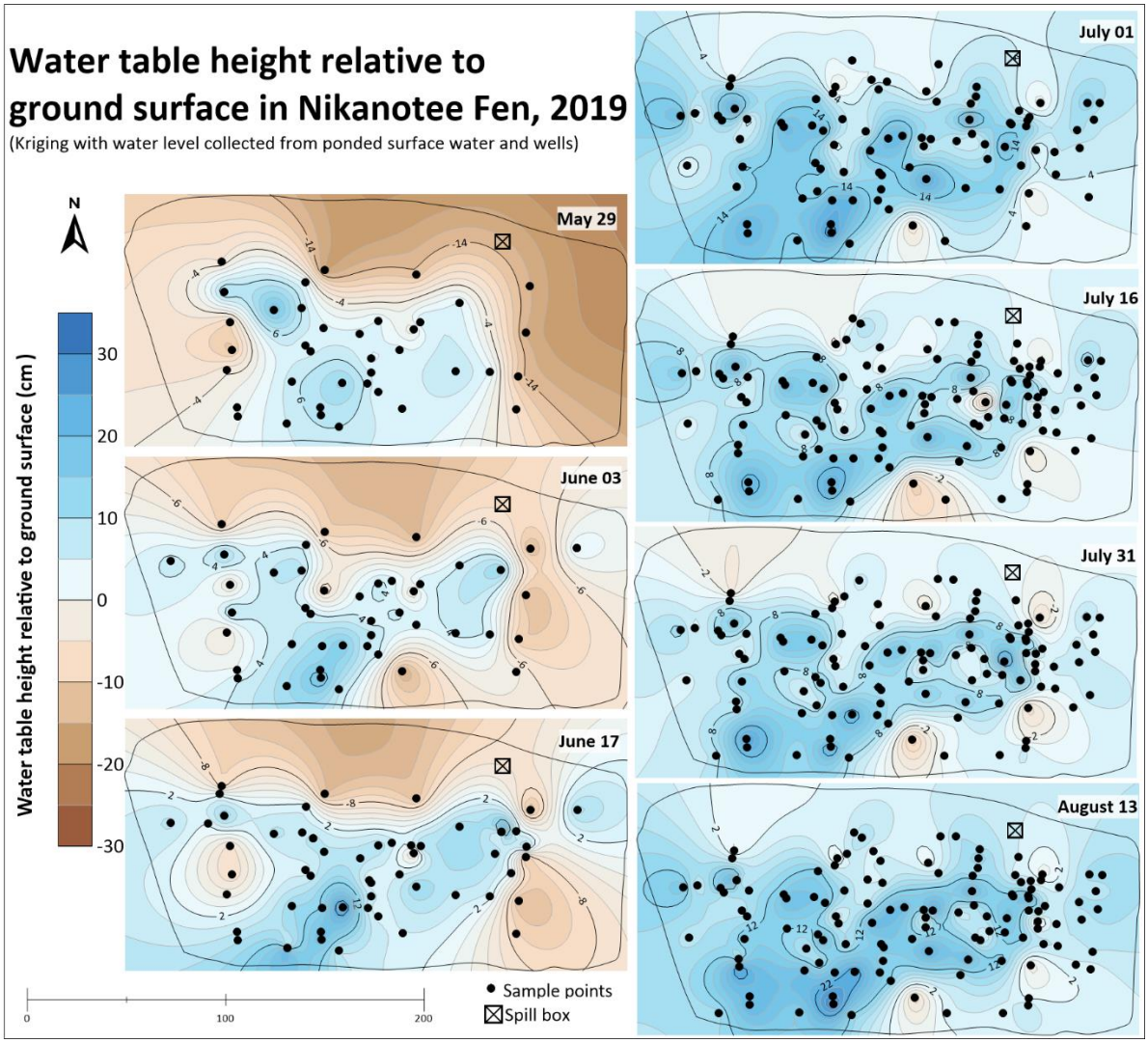

Figure 3-6 Water table height contours in cm relative to ground surface shown for a dry period (May to June) and a wet period (July to August).

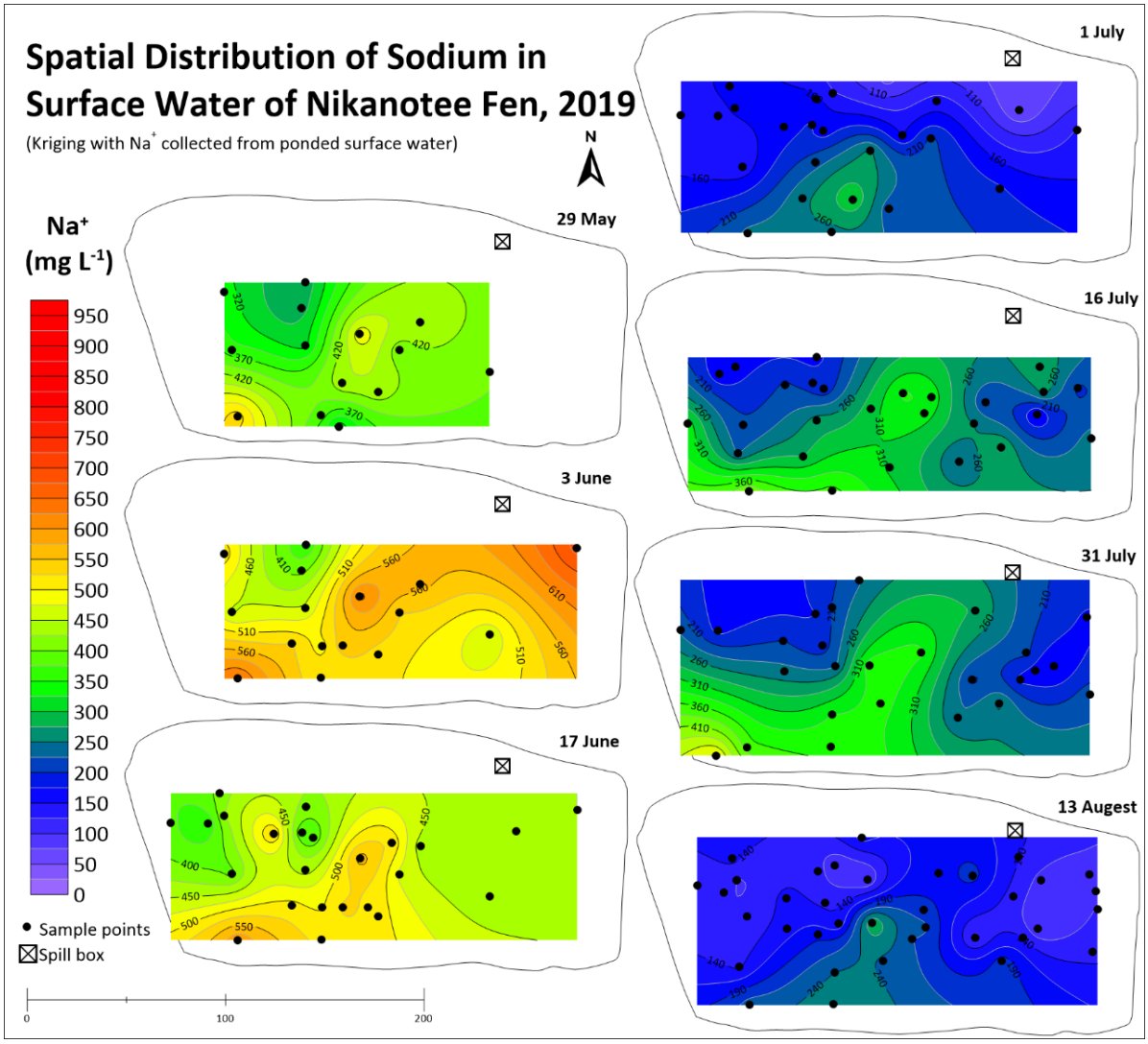

Figure 3-7 Spatial distribution of sodium concentrations interpolation in surface water at Nikanotee Fen, 2019. May and June were considered as dry period; July and August were considered as wet period.

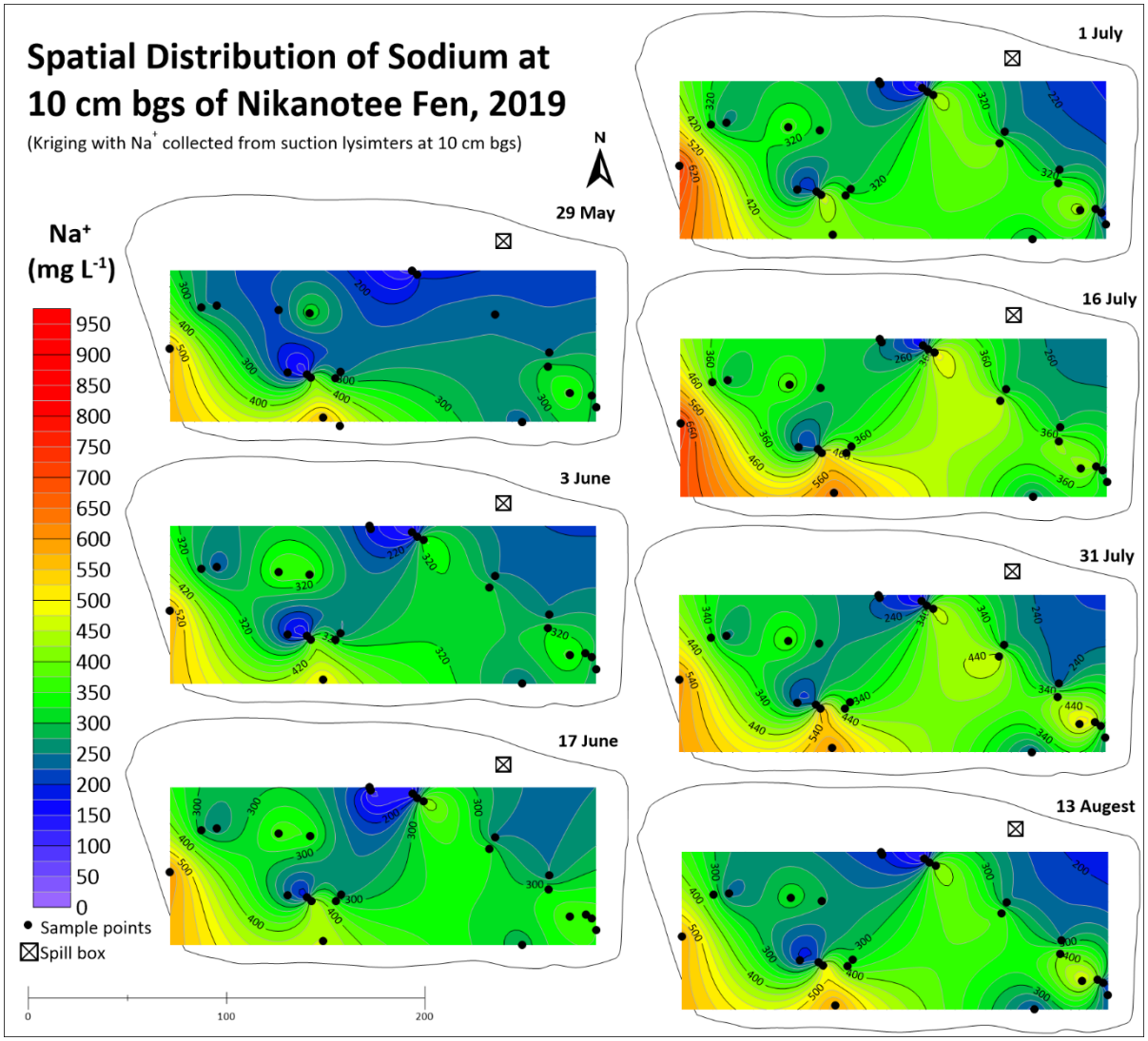

Figure 3-8 Spatial distribution of sodium concentrations at 10 cm bgs in Nikanotee Fen, May 29th – August 13th, 2019.

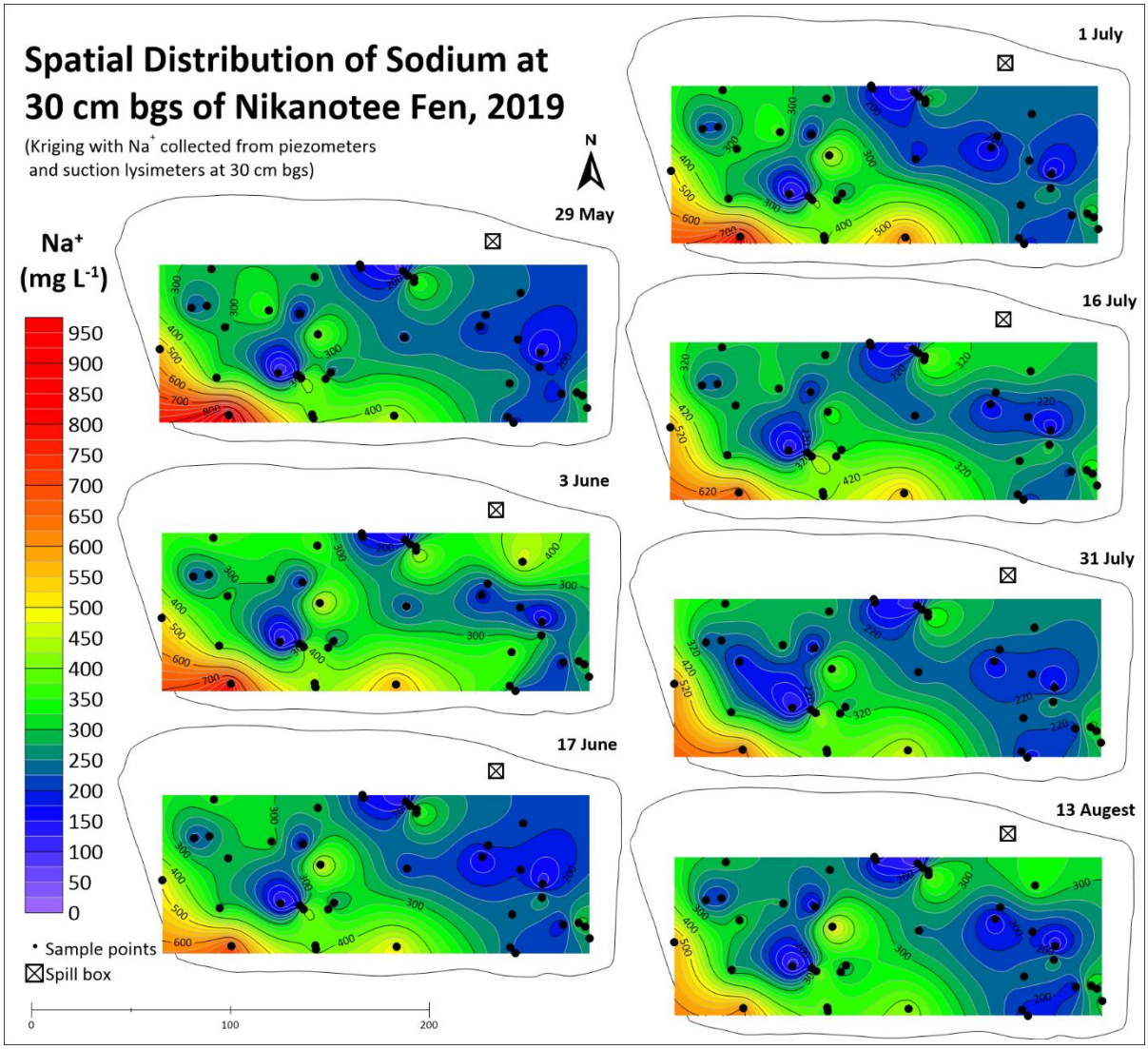

Figure 3-9 Spatial distribution of sodium concentration at 30 cm bgs in Nikanotee Fen, 29th – August 13th, 2019.

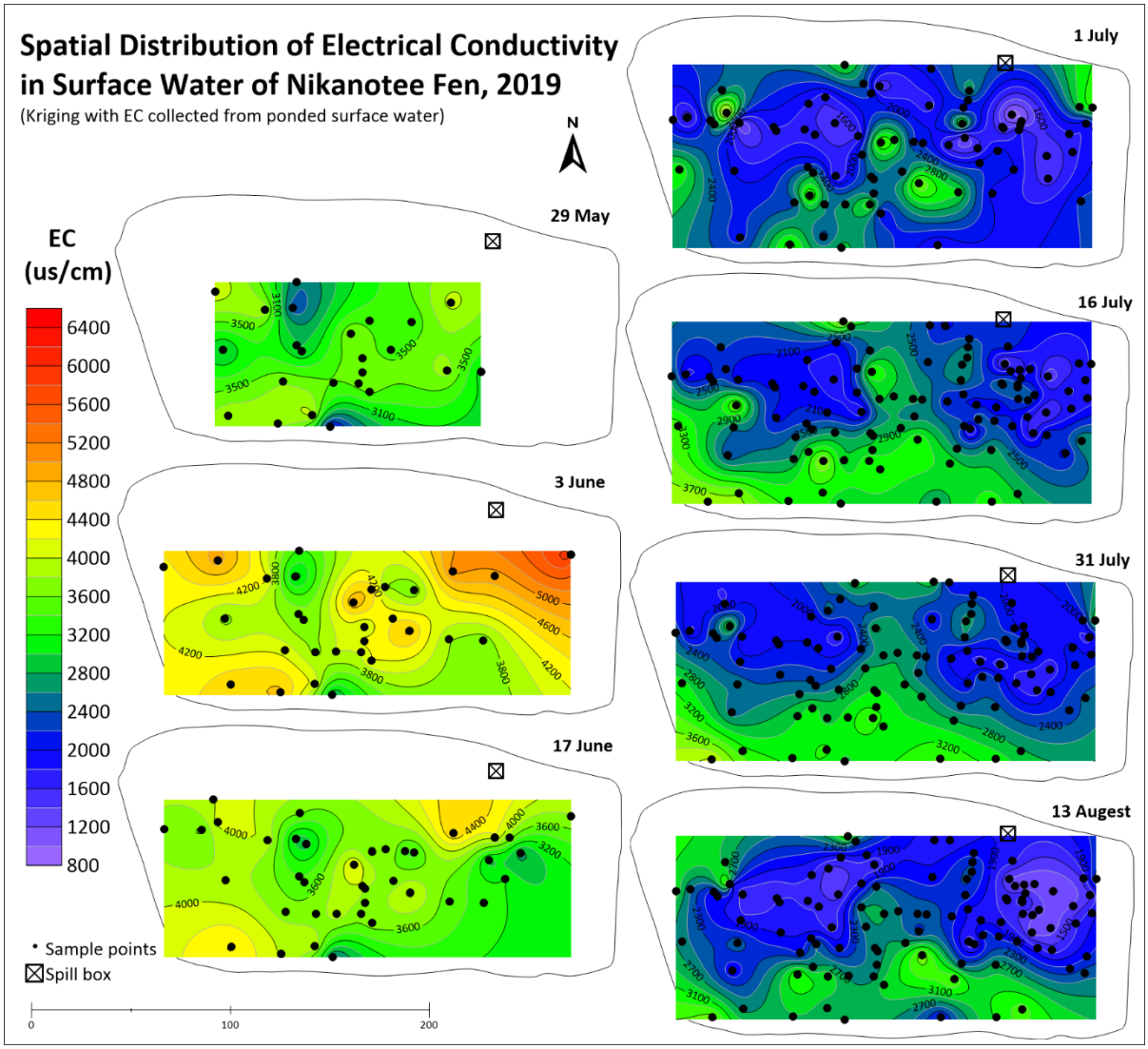

Figure 3-10 Spatial distribution of EC in ponded surface water at Nikanotee Fen, 29th – August 13th, 2019.

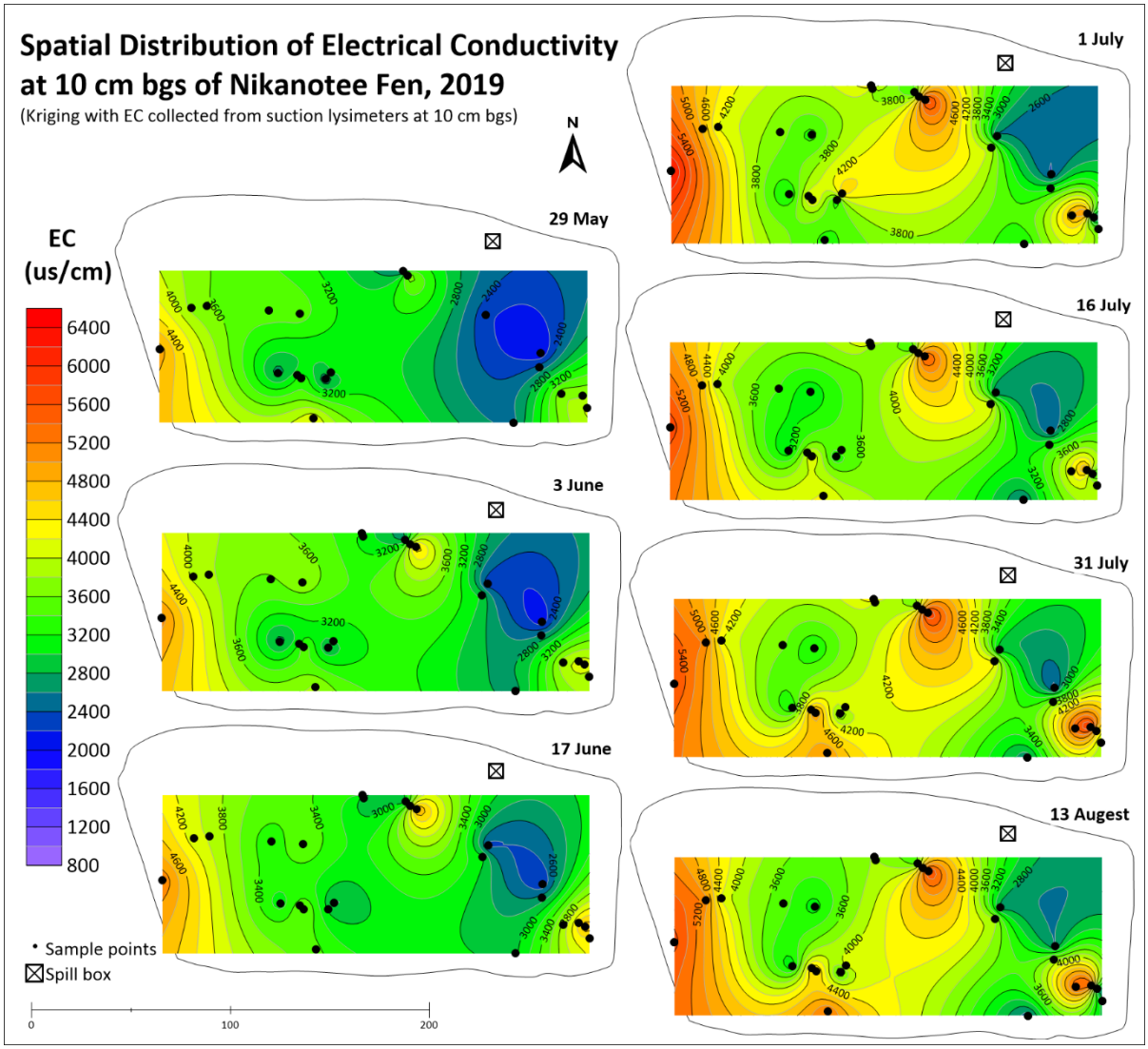

Figure 3-11 Spatial distribution of EC at 10 cm bgs in Nikanotee Fen, 29th – August 13th, 2019.

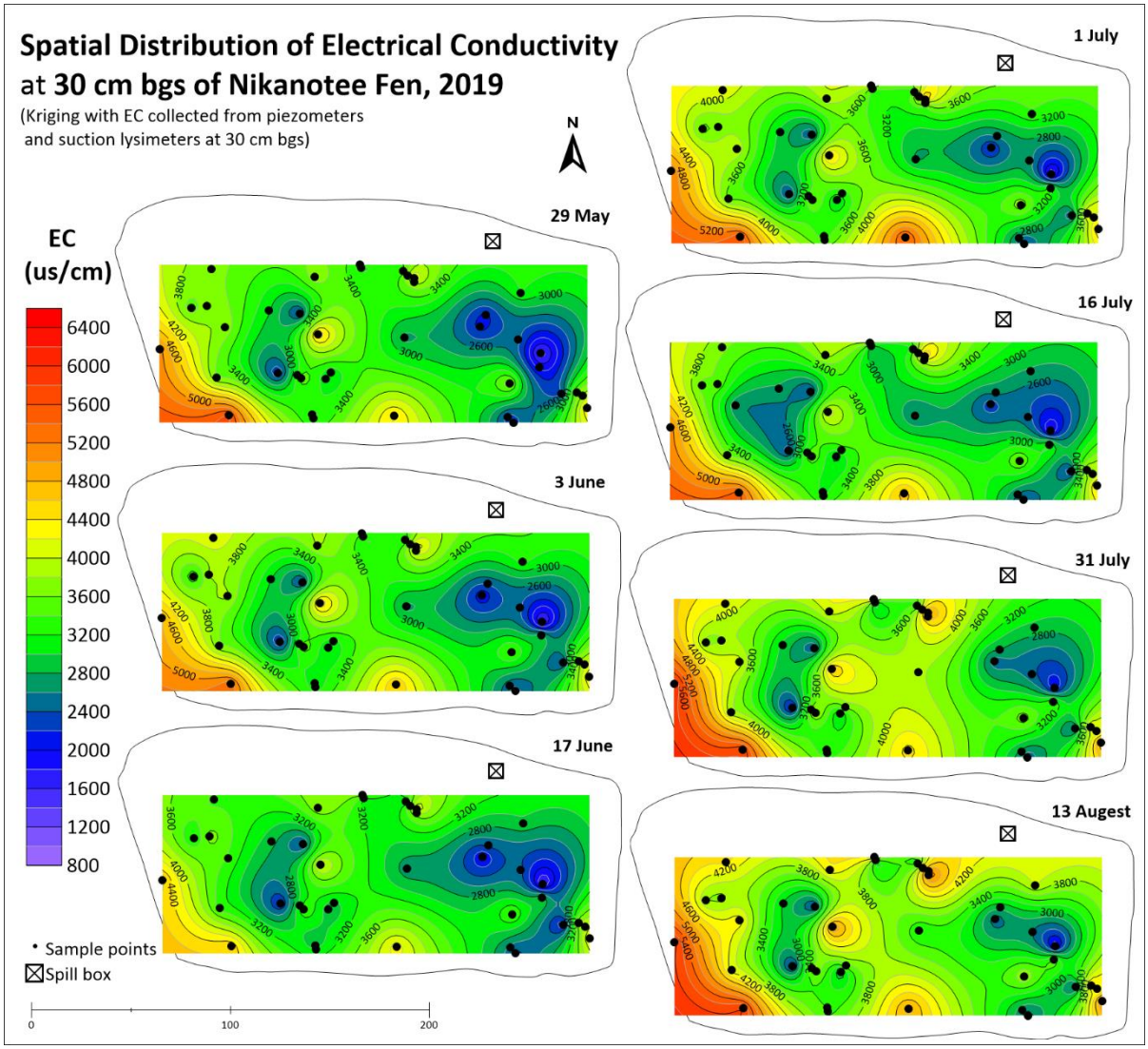

Figure 3-12 Spatial distribution of EC at 30 cm bgs in Nikanotee Fen, 29th – August 13th, 2019.

3.4 Mass balance

In the unsaturated and saturated part of the peat profile, the Na^+ mass is determined for the proportion of water in the peat; the seasonal average θ for the unsaturated zone (at 2.5, 5, 10, & 15 cm bgs) on sampled dates in 2019 was 0.85 (Table 3-4). In the saturated zone the proportion of water is represented by the average porosity for peat (0 – 50 cm), which at this site was reported to be 0.92 (Kessel et al., 2018).

Table 3-4 Seasonal average of volume (V), Na^+ concentrations (C), and volumetric water content (θ), measured in the field during the study period, with porosity previously measured by Kessel et al. (2018).

Parameter	V (m^3)	C (mg L^{-1})	θ (%)
Surface water	1315	289	-
Unsaturated peat	249	324	0.85
Saturated peat	7639	286	0.92[a]

[a] Values from (Kessel et al., 2018)

Table 3-5 Sodium mass estimation for each sampling events (unit in kg)

Date range	Days	Ponded surface water column	Unsaturated peat [a]	Saturated peat [a]	Total mass stored	Mass change in storage	Surface discharge	Groundwater inflow [b]
		Na_{water}	Na_{unsat}	Na_{sat}	Na_{Tot}	ΔNa_{Tot}	M_Q	M_{GW}
03/06	-	229	177	2323	2728	-	-	-
03/06 to 17/06	15	339	140	2119	2598	-130	44	-99
18/06 to 01/07	14	337	2	2436	2774	176	43	34
02/07 to 16/07	15	373	20	2423	2815	40	59	35
17/07 to 31/07	15	372	17	2265	2654	-160	59	54
01/08 to 13/08	13	369	3	2290	2663	8	55	58
Average	-	336	60	2309	2705	-	-	-
Seasonal change	72	140	-174	-33	-66	**-66**	**261**	**82**

All values are expressed with respect to the total cell area (2.3 ha).
[a] Total thickness of peat in this study is 35 cm.
[b] Seasonal average upward groundwater flux, $GW = 0.24\ mm\ day^{-1}$

The Na^+ mass balance for the top 35 cm of fen peat between each sampling event period is reported in Table 3-5. Average total Na^+ mass (Na_{Tot}) stored in ponded surface water and pore water in peat was 2705 kg in 2019. Average Na^+ estimated in the water column, unsaturated peat layer and saturated peat (top 35 cm of peat) layer of the fen were 336 kg, 60 kg, and 2309 kg, respectively. At the beginning of the season, the sampling event conducted on June 3rd showed the estimated Na^+ mass total was 2728 kg, then gradually decreased to 2663 kg at the end of the study period, except for a increase on July 1st, July 16th and August 13th (+ 176, +40 and +8 kg, respectively; Table 3-5 & Figure 3-13). The Na^+ mass estimated in the ponded surface water was the lowest in the early season (229 kg on June 3rd), and higher in the late season (373 kg on July 16th). In the unsaturated zone of peat, the Na^+ mass was found higher in June (> 140 kg), and one or two orders of magnitude lower in July and August (2 ~ 20 kg). In the subsurface saturated zone (top 35 cm of peat), the highest Na^+ mass was found on July 1st (2436 kg) and the lowest was found on June 17th (2119 kg).

In conclusion, the right side of Eq.6, in which Na^+ mass balance was estimated from the hydrological fluxes was $-179\ kg$ from June 3rd to August 13th, 2019, calculated from total Na^+ mass input via groundwater $M_{GW} = 82\ kg$ and total Na^+ mass leaving the system via surface discharge $M_Q = 261\ kg$ (Table 3-5). For comparison, the left side of Eq.6, in which Na^+ mass was estimated from the change in storage of Na^+ in ponded surface water and subsurface peat for the same period was $\Delta Na_{Tot} = -66\ kg$ (Table 3-5); the residual represents the error term, $\varepsilon = -113\ kg$, is ~ 63% of the estimated change in mass.

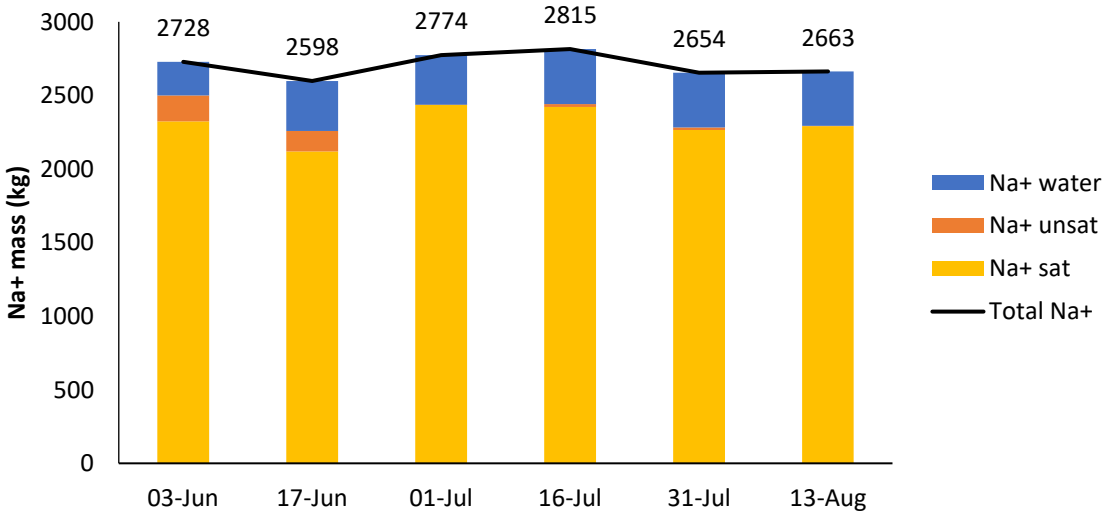

Figure 3-13 Na^+ mass (kg) estimated in ponded surface water layer (Na^+ water), unsaturated peat layer (Na^+ unsat) and saturated peat layer (Na^+ sat), for the zone above 35 cm bg, for each sampling events.

3.4.1 Additional Na^+ mass estimation

In 2019, the estimated Na^+ mass in the fen peat (0 ~ 200 cm bgs) and ponded surface water was 8.8 tones (Appendix F). At the end of the season (i.e., outside the mass balance period), large rainfall events occurred on August 16th (38 mm) and August 22nd (15 mm, Figure 3-1 (a)). *Q* increased rapidly from 0.2 L s^{-1} on August 15th to 0.5 L s^{-1} on August 16th (Figure 3-1 (c)). *Q* continued to rise to 0.6 L s^{-1} the next day and remained above 0.35 L s^{-1} until August 28th, with a second peak of 0.5 L s^{-1} on August 22nd (Figure 3-1 (c)). On the contrary, Na^+ concentration decreased from 290 mg L^{-1} on August 15th to 148 mg L^{-1} on August 16th and followed an almost symmetrical trend to that found in discharge rate (Figure 3-1 (c)). The Na^+ mass estimated in discharge from August 14th to August 31st (in total of 17 days) was 116 kg, which was not included in the Na^+ mass balance because Na^+ concentration in ponded water and shallow subsurface zone were not measured after August 13th, thus, Na^+ mass change in storage after this date cannot be calculated. This is nearly half of the total change observed between June 3rd and August 13th.

Chapter 4
Discussion

4.1 Hydrological pathways for Na^+

The driving force for groundwater flow in the Nikanotee Fen watershed was precipitation-driven recharge in the upland, which flowed up from under the fen due to the combination of groundwater mounding in the upland, sloping underlying geo-synthetic liner beneath the system, petroleum coke underdrain, and high evaporative demand at the fen surface (Ketcheson et al., 2017). The 2019 study period (May 18th to August 31st) was a relatively cool and wet season relative to the 1981 to 2018 normals (Appendix D). The 2019 study period had higher precipitation (264 mm; +25%) and lower evapotranspiration (272 mm; -18%) compared to values for this period from 2013 to 2018 (Table D. 1). In the water budget, the fluxes showed a net loss (-43 mm), but the storage change showed an increase (60 mm) in the system. This residual error (-103 mm) is potentially explained by the groundwater underestimation due to vertical hydraulic gradient measurement error under wet and cool weather conditions. The estimated hydraulic gradients (Figure I-1) were very different from those reported by Kessel et al., (2018) for this site between 2013 and 2016, which ranged from 0.011 – 0.015. A larger and consistently upward hydraulic gradient would have dramatically reduced the residual error of the water budget. Here, GW inflow (26 mm) was much less than previously reported (Ketcheson et al., 2017; 177 mm in 2014).

The initial average Na^+ concentration measured within the ponded water and subsurface peat pore water of the fen was ~304 mg L^{-1} in the frozen period (Table 3-2). Na^+ became mobile with snowmelt mixing with surface water and pore water. In the dry period, small but infrequent *P* and consistent *AET* resulted in a slight increase in Na^+ concentration in ponded and subsurface water to ~341 mg L^{-1} (Table 3-2). Na^+ concentration and EC measured in ponded surface water quickly responded to precipitation and evapotranspiration in the wet period (Figure 3-1, Figure 3-5, Figure 3-7, & Figure 3-10), as precipitation diluted Na^+ concentration, whereas evapotranspiration removed water vapor from the system and resulted in an increasing Na^+ concentration at or near the surface (evapo-concentration). Following the first substantial rainfall event in late June (28th), Na^+ concentration from ponded surface water decreased from 461 to 181 mg L^{-1} (61% decrease, Figure 3-1 (b)). To determine if this rainfall (*P* = 68 mm between June 28th and July 1st) can explain the observed dilution in ponded surface water, a set of calculations were made (Appendix E). Using this approach this amount of dilution could be achieved with only 53 mm of rain. During this period, the additional water from rainfall increased the average water depth by 3.7 cm in the ponded surface water, which also increased

the ponded water surface area, and explains why the actual rainfall (68 mm) did not provide additional dilution. Furthermore, it is possible that Na^+ was redistributed from adjacent drier areas.

A relatively dry period with infrequent and less intense rainfall in early July resulted in a slight increase in Na^+ concentration in the surface (Figure 3-1 (b)). Following this, concentration further decreased with more frequent and intense rainfall in August (to 156 mg L^{-1}, Figure 3-1 (b)). However, Na^+ concentration and EC measured from 10 and 30 cm bgs were less sensitive to the precipitation and evapotranspiration, given that their spatial and temporal pattern did not change much over the study period (Figure 3-1 (b), Figure 3-8, Figure 3-9, Figure 3-11 & Figure 3-12); the slower change reflects the slower mixing of porewater as water infiltrate to deeper peat, compared to surface water. The observed pathway of elevated Na^+ and EC appearing in the central part of the fen trending towards the spill box (from south-west to north-east, with lower elevations) could be a result of the discharge of ponded surface water and that in the top 10 cm bgs (Figure 1-2 (b), Figure 3-7, Figure 3-8, Figure 3-10 & Figure 3-11).

In 2019, Na^+ concentration and EC found in peat at 50 cm bgs was 236 ± 148 mg L^{-1} and 3641 ± 926 µS cm^{-1}, respectively (Table 3-3), which increased since 2016 from that found in peat at 50 cm bgs (200 ± 126 mg L^{-1} and 3570 ± 1580 µS cm^{-1}, respectively; Kessel et al., 2018). The Na^+ concentration was anticipated to increase season-over-season, at least in the short-term (Kessel et al. 2018, Simhayov et al. 2017). The "hotspots" of Na^+ concentration and EC – areas of particularly high concentrations – were found near the south-west of the fen, whereas the lower values were observed near the north and east of the fen (Figure 3-7 ~ Figure 3-12). A possible explanation for this is that the water table was constantly above ground surface in the south-west corner (Figure 3-6), and thus the evapotranspiration rate was highest there (4.4 mm day^{-1}), which is slightly higher than it was in seedlings plots (3.9 mm day^{-1}) that occur mostly near the north and east of the fen (Scarlett et al., 2017). Higher evapotranspiration would thus lead to increased Na^+ (and EC) accumulation and evapo-concentration in the ponded area near the south-west of the fen. This pattern could also be a consequence of the spatial patterns of groundwater flow from upland to fen across the transition zone and through the petroleum coke, which ultimately transports Na^+ through the peat column (Figure 2-7). Specifically, these nested groundwater flow paths will result in earlier arrival of Na^+ near the surface of the fen directly adjacent to the transition zone, while the distal areas of the fen (northern and western) will have later arrival of upland groundwater, and generally less effective surface flushing (Sutton and Price, in prep). Furthermore, at the Nikanotee Fen, higher hydraulic gradients driven by the presence of preferential recharge features on the eastern side of the upland in conjunction with the position of

the spill box on the eastern side of the fen contribute to an earlier appearance of salinity at the surface compared to the distal fen areas (Kessel et al., submitted).

In 2019, average Na^+ concentration found in the top 35 cm of peat in the fen was 292 mg L^{-1}. Meanwhile, average Na^+ concentrations from peat at 50, 90, and 150 cm bgs were 236, 145, and 139 mg L^{-1}, respectively. Thus, there was a trend of increasing Na^+ concentrations towards the surface in the fen (Figure 3-3). Sutton and Price (in prep.) showed a similar trend for parts of the fen for 2018. Simhayov et al. (2017) showed with laboratory experiments and modeling that evapo-concentration can sharply increase near-surface Na concentrations in peat from the constructed fen. Evidently, some of this Na^+ has accumulated to depth of 50 cm in the fen. More investigation on solute transport within the fen, and the role of evapo-concentration is recommended.

4.2 Na^+ mass balance comparison

Na^+ mass estimated in the fen and upland portions of the Nikanotee Fen Watershed at its inception was 27 tonnes, of which 0.6 tonnes were in fen peat (Simhayov et al. 2017). Na^+ mass contained in the upland has gradually moved to the fen, such that the estimated Na^+ mass in fen peat (0 ~ 200 cm bgs) and ponded surface water had increased to 8.8 tonnes by 2019 (Appendix F). Kessel (2016) estimated saturated zone Na^+ mass totals in peat (0 – 70 cm) of the fen to be ~ 3 tonnes (or 0.15 kg m^{-3} of peat) on July 16th, 2015. In the current study, using a similar approach but for the top 35 cm saturated peat, Na^+ mass was estimated to be 2.4 tonnes (or 0.31 kg m^{-3} of peat) on July 16th, 2019, which is much higher per unit volume of peat than it was four years previously. In 2019, Na_{water} and Na_{unsat} were found to be higher in the dry period and lower in the wet period; on the contrary, Na_{sat} was lower in the dry period and higher in the wet period, in response to water level increase after rainfall. The total Na^+ mass change ΔNa_{Tot} of ponded surface water and subsurface peat (0 – 35 cm) indicated the system lost 66 kg over the mass-balance period (June 3rd to August 13th). Na^+ has accumulated in the rooting zone (top 30 cm), which Prystupa (2020) showed to increase DOC concentration in the peat, and which can cause less salt-tolerant vegetation to experience salt stress (Rezanezhad et al. 2012, Trites and Bayley, 2009). However, the loss of 206 kg Na^+ mass estimated in the shallow subsurface zone of peat (unsaturated and saturated) suggested that the Na^+ mass might be re-distributed to surface ponds (seasonal increase of 140 kg) and leave the system via discharge at the spill box. The hydrological component in water balance and in Na mass balance are both showing a net loss in the system. For the frost-free period (June 3rd to August 13th), the water balance showed a net loss of water from hydrological components (-38 mm), yet the change in water storage showed an increase of 41 mm (Table 3-1). This was likely due to underestimation of groundwater flux from the upland aquifer to the fen (177 mm in 2014, Ketcheson et al., 2017, see Appendix H for limitations).

The Na^+ mass estimated from hydrological fluxes ΔM was -179 kg, which was larger than ΔNa_{Tot} (-66 kg). The residual was -113 kg, which represents the mass balance error. As previously noted for the water budget, groundwater inflow was probably substantially underestimated. If previously reported values of vertical hydraulic gradient (Kessel et al., 2018) had been used to estimate the groundwater influx, the Na^+ mass balance residual would have been much smaller.

In most years, Na^+ was redistributed within the system by groundwater (Kessel et al., 2018), which generally moves from petroleum coke upwards to peat (Ketcheson et al., 2017). However, the seasonal average vertical hydraulic gradient between the petroleum coke and peat in 2019 was in a downward direction, albeit close to zero (seasonal average of -0.00087). This net downward direction was likely due to the relatively wet and cool season, which led to ponding on the surface of the fen which countered the more typical upward trend (Ketcheson et al., 2017). It is acknowledged that the small gradients exacerbate the importance of measurement error, which associated with manual water table and hydraulic head measurements (±0.5 cm) are comparatively large when considering a hydraulic head difference of (<1 cm) between the petroleum coke and fen water table. Despite this seasonal average hydraulic gradient being negative (downwards), the total Na^+ mass in groundwater flux to the fen, $M_{GW,}$ was estimated to be 82 kg over the study period. Seasonal average Na^+ concentration found in surface discharge measured at the v-notch was 228 mg L^{-1} (± 66 mg L^{-1} standard deviation), which is slightly lower than that found in the fen surface and subsurface (292 ± 129 mg L^{-1}). This could be a result of Na^+ redistribution flushing to the spill box or dilution of surface water mixing with lower concentration water from the precipitation-driven discharge. Na^+ discharge from the spill box, M_Q, removed approximately 261 kg of Na^+ over the 72-day studied period (average of 3.6 kg day^{-1}). Approaching the end of the season (not included in the mass balance), two relatively large rainfall events (38 mm and 15 mm) produced a rapid increase of discharge (0.2 to 0.6 L s^{-1}). Although the Na^+ concentration measured in discharge was reduced, the higher flow rate resulted in greater loss (116 kg of Na^+ mass over 17 days, with an average of 6.8 kg day^{-1}), compared to that in the early wet period (average of 3.6 kg day^{-1}). Large rainfall events might be responsible for exporting increased loads of Na^+, which will flush Na^+ from the fen but could affect down-gradient landscapes. Thus, precipitation frequency and magnitude are important components to investigate Na^+ export and to predict the flushing timeframe. In the long term, Na^+ from upland tailings sand will migrate to the fen peat and leave the system though the spill box. Plant uptake of Na^+ mass was not included in the Na^+ mass balance calculation, however, consideration and investigation on using living plants to remove, transfer, stabilize and/or destroy contaminants in soil (phytoremediation) is recommended in future reclamation design.

Given relatively cool and wet years similar to conditions in 2019, a total mass of 27 tones Na^+ originally determined for the newly constructed fen-upland system (Simhayov et al. 2017), discharging at 4 kg day^{-1} in the study period (a total of 429 kg of Na^+ discharged in 106 days from May 18th to August 31st), the approximate time for Na^+ to leave the Nikanotee system is 36 frost-free periods (typically 183 days each year), or 6672 days total. However, one-year's observation of the Na^+ concentration in discharge is not sufficient to predict this flushing timeframe. In the cool and wet 2019 season, it caused more than typical release of sodium, and mass export will decrease asymptotically in the future, so the timeframe for Na^+ to leave the system could be longer. Future studies to monitor Na^+ concentration in discharge is also recommended.

4.3 Potential sources of errors

Care was taken to minimize errors when conducting in-field manual measurements, including water level and discharge from the fen outflow. However, 12 out of 312 water level measurements were missing due to weather conditions especially during frozen period. The implications of this error were likely small as the record was gap-filled with nearby nests. Certain areas such as the persistent ponds were inaccessible, which may have had a stronger and more consistent evaporative signature. Therefore, the surface water that was capable of being sampled in the field would perhaps bias the results towards a diluted signature. Additionally, surface and pore water sampling events for Na^+ concentration were not repetitive at the same points. The number of sampled points were different each time. The thickness of ponded surface water was estimated using all sampling points to minimize the bias. Initial Na^+ concentration was measured with Orion probe in a field-lab setup. It was then validated with Dionex measurement on selected samples after the field season. Uncertainty arises from using the correlation ($R^2 = 0.97$) between these two methods.

The sample size for the original design of this study was relatively small and highly dependent on water availability in ponded areas. The water table contours in the dry period could be biased due to lack of surface water depth measurement at the north-east corner when there was not enough surface water available to measure. Furthermore, although data collected by lysimeter extraction was added to increase the sample size, water table fluctuation could result in a situation that some tensiometers were collecting pore water from unsaturated zone, yet some were in the saturated zone thus included in Na_{sat} when available. The use of data interpolation contouring tools to illustrate the spatial and temporal distribution of Na^+ concentration and EC magnifies the uncertainty due to the sample size and sparse sampling locations. The interpolation was missing for places where limited water was available for sample collection. Water samples collected from discharge were also highly dependent on the water availability. Na^+ concentration in surface discharge was estimated using logged EC validated with

manually collected discharge samples. If the surface discharge was too low to flush out through the v-notch, the EC logged could be just stagnant water behind the v-notch. Meanwhile, water seepage was collected less frequently, thus, the Na^+ mass estimated in discharge might be under-estimated. Therefore, the residual error of Na^+ mass balance was high (~63%).

The estimates of vertical hydraulic gradient were not consistent with previously published measured values (Ketcheson et al., 2017; Kessel et al., 2018), nor modelled seasonal values (Sutton, 2021), which all showed a more consistent and stronger upward gradient. This led to a likely underestimate of groundwater inflow in the water budget, hence underestimate of Na^+ influx in the mass balance.

Chapter 5
Conclusion

This study assessed the near surface distribution, transport, and export of Na^+ within the Nikanotee Fen within the 7th year post-construction. In general, Na^+ concentration and EC measured in ponded surface water steadily increased due to high evapotranspiration but was sensitive to freshwater inputs (rainfall), which caused variability in concentration and redistribution primarily through surface ponds. Na^+ concentration decreased as precipitation introduced fresh water, resulting in dilution (61% and 40% reduction in Na^+ concentration and EC, respectively, in response to June 28th rainfall) and increased as evapotranspiration removed water but not solute from the system, resulting in evapo-concentration. On the contrary, these processes had little influence on Na^+ concentration and EC measured at 10 and 30 cm bgs, which remained fairly consistent, with only a slight increase over the study period. This suggests that the process of dilution is subtle and requires intentional monitoring and consideration in hydro-chemical studies or modelling. Even shallow pore-water samplers (such as 10 cm bgs) were unable to illustrate the dynamics of near-surface Na^+ concentrations or EC. This has further implications for the growth, productivity, and survival of mosses, which usually exhibit low salinity tolerance (Boerner and Forman, 1975). The salinity of water closest to the surface will have the dominant influence on moss productivity given the non-vascular nature of bryophytes. Since mosses such as: T. Nitens, S. Warnstorfii, etc. are regionally abundant peat-forming species in many fens (Batzer & Baldwin, 2012), and which are targeted for inclusion into reclaimed wetlands, the water chemistry of ponded surface water should be studied in detail.

The highest Na^+ concentration and EC were found near the south-west corner, where it was the wettest over time with ponded surface water (seasonal average of water table at 16 cm ags). In contrast, the lowest Na^+ concentration and EC were found near the north-east corner, where it was relatively dry over time (seasonal average of water table at 1.5 cm bgs) and closest to the discharge point of the fen. A trend of higher Na^+ concentration and EC from the centre of the fen towards the spill box was observed in the surface as a result of lower elevation ponds and preferential flow to the spill box outflow. The seasonal average Na^+ concentration and EC at the surface in 2019 has increased compared to those found near the surface in previous years. Na^+ has reached to the rooting zone of the fen, which could shift the vegetation there to a more salt-tolerant species.

To identify and quantify components of the Na^+ mass balance in ponded surface water and shallow subsurface zone of the fen, the balance was calculated by Na^+ mass measured in storage and within hydrological pathways. The change in Na^+ mass measured in storage was estimated from

samples collected in ponded surface water and subsurface peat of the fen, which was -66 kg over the studied period. Within that, 140 kg of Na^+ was entered into ponded surface water, and 206 kg of Na^+ was removed from subsurface peat, which might have been re-distributed into and within peat, taken up by vegetation, or discharged through spill box. The hydrological component in water balance and in Na mass balance are both showing a net loss in the system. For the frost-free period (June 3rd to August 13th), the water balance showed a net loss of water from hydrological components (-38 mm). When estimating Na^+ mass within hydrological pathways, the potential fluxes influencing Na^+ transport include groundwater inflow, precipitation, inflow from hillslope runoff, streamflow discharge from the fen, and evapotranspiration. Plant uptake of Na^+ mass was not included in the Na^+ mass balance calculation in this study, however, phytoremediation can be considered in future reclamation design. This study focused on Na^+ mass within groundwater and discharge because Na^+ concentration found in precipitation, hillslope runoff entering the constructed system, and evapotranspiration were 2 orders of magnitude lower than values found in groundwater and discharge. The vertical hydraulic gradient between petroleum coke underdrain and peat in 2019 was 2 orders of magnitude lower than previous years' (average ~0.013 between 2013 and 2016) because it was a relatively wet and cool year. Thus, the groundwater input was estimated to be 82 kg, which was likely underestimated due to measurement error. The estimated change in Na^+ mass within hydrological pathways was -179 kg over the studied period (net loss). The estimated change in Na^+ mass sampled in ponded surface water and shallow subsurface peat was also showing a net loss of 66 kg.

Ultimately, Na^+ from upland tailings sand will migrate to the fen peat and potentially leave the system though discharge. The estimated Na^+ mass leaving the system was 4 kg day^{-1} through discharge over the frost-free period. Based on the assumption of similar meteorological conditions to those in 2019, the approximate time for Na^+ to leave the Nikanotee system is about 36 frost-free periods (36 years or 6672 days) post-construction. The actual time will vary depending on actual weather conditions. Future studies to monitor Na^+ concentration in discharge is recommended because the timeframe of this research was for a single growing season, and therefore the impact of differing meteorological conditions on surface concentration and sodium mass export is speculative.

This study has assessed the temporal variation and spatial distribution of Na^+ concentrations and EC within the surface water and the shallow subsurface zone, as well as identified and quantified components of Na^+ mass balance and water balance of hydrological processes governing the movement of salt at the constructed fen. This work has implications for peatland construction as a part of reclamation. Furthermore, areas for future research have been identified to better assess the Na^+ in peatlands and in the constructed fen specifically. Namely, more investigation on solute transport within

the fen (e.g., plant uptake), and the role of evapo-concentration is recommended. The process of dilution and concentration should be intentionally monitored and considered in hydro-chemical studies or modelling to address the sensitive response at surface. Fen discharge as the major pathway for Na^+ removal in the constructed fen suggested that reclamation design should frequently and consistently monitor discharge water quantity and quality to refine the flushing timeframe prediction.

Bibliography

Alberta Environment and Sustainable Development. (2015). *Alberta wetland classification system*.

Batzer, D. P., & Baldwin, A. H. (Eds.). (2012). *Wetland habitats of North America: ecology and conservation concerns*. University of California Press.

Boerner, R. E., & Forman, R. T. (1975). Salt spray and coastal dune mosses. *Bryologist*, 57-63.

Daly, C., Price, J., Rezanezhad, F., Pouliot, R., Rochefort, L., & Graf, M. D. (2012). *Initiatives in oil sand reclamation: Considerations for building a fen peatland in a post-mined oil sands landscape* (pp. 179–201). pp. 179–201. Retrieved from http://www.gret-perg.ulaval.ca/uploads/tx_centrerecherche/Daly_etal_2012_Restoration_Chapter_03.pdf

Freeze, A. R., & Cherry, J. A. (1979). *Groundwater.* Prentice-Hall.

Golden Software (2020). *A Basic Understanding of Surfer Gridding Methods – Part 1*. Retrieved from https://support.goldensoftware.com/hc/en-us/articles/231348728-A-Basic-Understanding-of-Surfer-Gridding-Methods-Part-1#

Golden Software (2019). *Surfer Full User's Guide.* Retrieved from http://downloads.goldensoftware.com/guides/Surfer17UserGuide.pdf

Gorham E (1991) *Northern peatlands: role in the carbon cycle and probable responses to climatic warming*. Ecol Appl 1:182–195. doi: 10.2307/1941811

Government of Alberta, (2017). *Oil Sands Mine Reclamation and Disturbance Tracking by Year*. Retrieved from http://osip.alberta.ca/library/Dataset/Details/27

Government of Canada. (2019). Station results - Historical data. Fort McMurray.

Hintze, J., & Nelson, R. (1998). *Violin Plots: A Box Plot-Density Trace Synergism.* The American Statistician, 52(2), 181-184. doi:10.2307/2685478

Kessel, E. D. (2016). *The Hydrogeochemistry of a Constructed Fen Peatland in a Post-Mined Landscape in the Athabasca Oil Sands Region, Alberta, Canada*. University of Waterloo Space. https://doi.org/10.1017/CBO9781107415324.004

Kessel, E. D., Ketcheson, S. J., & Price, J. S. (2018). *The distribution and migration of sodium from a reclaimed upland to a constructed fen peatland in a post-mined oil sands landscape.* Science of the Total Environment, 630, 1553–1564. https://doi.org/10.1016/j.scitotenv.2018.02.253

Kessel, E. D., Sutton, O.F., & Price, J. S. (2019). The use of recharge basins to modify the hydrology of a constructed tailings sand aquifer for oil sands reclamation and its implications on solute flushing. Manuscript submitted for publication.

Ketcheson, S. J., & Price, J. S. (2016a). *Comparison of the hydrological role of two reclaimed slopes of different ages in the Athabasca oil sands region, Alberta, Canada*. Canadian Geotechnical Journal, 53(9), 1533–1546. https://doi.org/10.1139/cgj-2015-0391

Ketcheson, S. J., Price, J. S., Carey, S. K., Petrone, R. M., Mendoza, C. A., & Devito, K. J. (2016b). *Constructing fen peatlands in post-mining oil sands landscapes: Challenges and opportunities from a hydrological perspective.* Earth-Science Reviews, 161, 130–139. https://doi.org/10.1016/j.earscirev.2016.08.007

Ketcheson, S. J., Price, J. S., Sutton, O., Kessel, E., Sutherland, G., & Petrone, R. M. (2017). *The hydrological functioning of a constructed fen wetland watershed.* Science of The Total Environment, 603–604, 593–605. https://doi.org/10.1016/j.scitotenv.2017.06.101

Kruskal, W. H., & Wallis, W. A. (1952). *Use of Ranks in One-Criterion Variance Analysis*. Journal of the American Statistical Association, 47(260), 583–621. https://doi.org/10.1080/01621459.1952.10483441

Messner LE, Hribljan, JA, Borkenhagen, AK, Strack M (in prep.) *Species introductions drive vegetation changes and biomass in a reclaimed fen, Oil Sand region, Alberta, Canada*.

National Wetlands Working Group. (1997). *The Canadian Wetland Classification System, 2nd Edition*. Warner, B.G. and C.D.A. Rubec (eds.), Wetlands Research Centre, University of Waterloo, Waterloo, ON, Canada.

Pouliot, R., Rochefort, L., & Graf, M. D. (2012*). Impacts of oil sands process water on fen plants: Implications for plant selection in required reclamation projects.* Environmental Pollution, 167, 132–137. https://doi.org/10.1016/j.envpol.2012.03.050

Price, J. S., McLaren, R. G., & Rudolph, D. L. (2010). *Landscape restoration after oil sands mining: Conceptual design and hydrological modelling for fen reconstruction*. International Journal of Mining, Reclamation and Environment, 24(2), 109–123. https://doi.org/10.1080/17480930902955724

Prystupa E, (2020). *Salinity Effects on Dissolved Organic Carbon Concentration and Quality in a Constructed Fen Peatland, Fort McMurray, AB.* UWSpace. http://hdl.handle.net/10012/16096

R Core Team (2013). *R: A language and environment for statistical computing. R Foundation for Statistical Computing, Vienna, Austria*. URL http://www.R-project.org/.

Rezanezhad, F., Andersen, R., Pouliot, R., Price, J. S., Rochefort, L., & Graf, M. D. (2012). *How fen vegetation structure affects the transport of oil sands process-affected waters.* Wetlands, 32(3), 557–570. https://doi.org/10.1007/s13157-012-0290-z

Scarlett, S. J., Petrone, R. M., & Price, J. S. (2017). *Controls on plot-scale evapotranspiration from a constructed fen in the Athabasca Oil Sands Region, Alberta*. Ecological Engineering, 100, 199–210. https://doi.org/10.1016/j.ecoleng.2016.12.020

Scarlett, S. J., & Price, J. S. (2019). *The influences of vegetation and peat properties on the hydrodynamic variability of a constructed fen, Fort McMurray, Alberta*. Ecological Engineering, 139(August), 105575. https://doi.org/10.1016/j.ecoleng.2019.08.005

Simhayov, R. B., Price, J. S., Smeaton, C. M., Parsons, C., Rezanezhad, F., & Van Cappellen, P. (2017). *Solute pools in Nikanotee Fen watershed in the Athabasca oil sands region.* Environmental Pollution, 225, 150–162. https://doi.org/10.1016/j.envpol.2017.03.038

Sumner, D. M., & Belaineh, G. (2005). *Evaporation, precipitation, and associated salinity changes at a humid, subtropical estuary.* Estuaries, 28(6), 844–855. https://doi.org/10.1007/BF02696014

Sutton, O. (2021). *Projecting the Hydrological and Geochemical Evolution of a Constructed Fen Watershed in the Athabasca Oil Sands Region, Alberta, Canada.* UWSpace. http://hdl.handle.net/10012/16965

Trites M, Bayley SE (2009) *Organic matter accumulation in western boreal saline wetlands: a comparison of undisturbed and oil sands wetlands.* Ecol Eng 35:1734–1742. doi: 10.1016/j.ecoleng.2009.07.011

Vitt, D., Halsey, L., Thormann, M., & Martin, T. (1996). *Peatland inventory of Alberta. Phase 1: Overview of peatland resources in the natural regions and subregions of the province., Centre PR (ed.)* University of Alberta.

Vitt D.H. (2006) *Functional Characteristics and Indicators of Boreal Peatlands*. In: Wieder R.K., Vitt D.H. (eds) Boreal Peatland Ecosystems. Ecological Studies (Analysis and Synthesis), vol 188. Springer, Berlin, Heidelberg. https://doi.org/10.1007/978-3-540-31913-9_2

Weinhold, B. (2011). *Alberta's oil sands: hard evidence, missing data, new promises*. Environmental health perspectives, 119(3), A126.

Wilcoxon, F. (1945). *Individual comparisons by ranking methods*. Biom. Bull. 1: 80–83.

Appendix A

Sodium probe validation

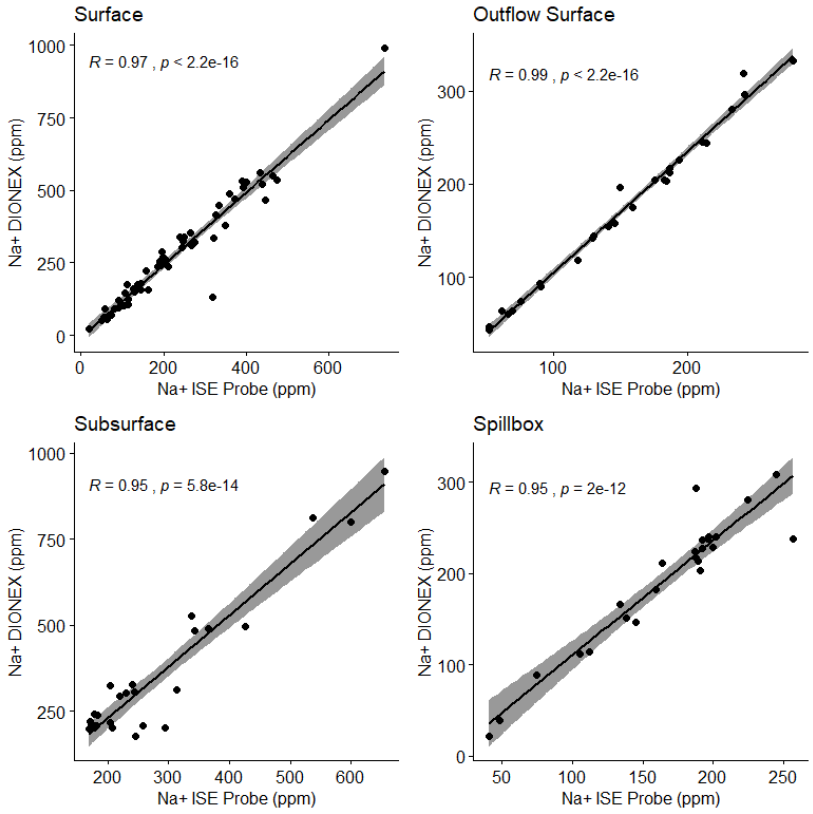

Figure A. 1 Sodium measured by Dionex ICS-1600 Method EPA 300.0 with AS-DV auto-sampler compared with sodium measured by Orion Star A324pH/ISE multiparameter meter with a ROSS Sodium Sure Flow Electrode (model 8611BNWP), using samples collected from surface ponded water (Surface), shallow subsurface fen (top 35 cm of peat, Subsurface), surface discharge (Outflow Surface), and subsurface discharge (Spillbox).

Equation $C_{Dionex} = 1.2 \times C_{Orion}$ was used to validate the Na^+ measured by Orion probe in the field.

Appendix B

Estimation for Na^+ concentrations in surface ponded water

Table B. 1 Summary table of area in each cell. Ponded surface area is the area of light blue shaded area (ponds) in Figure 2-6. Unsaturated area is the area of grey shaded area (dry surface) in Figure 2-6 (a). Cell area is the total of the two on each date.

Cell	Ponded area m^2						Unsaturated area m^2						Total cell area m^2
	03-Jun	17-Jun	01-Jul	16-Jul	31-Jul	13-Aug	03-Jun	17-Jun	01-Jul	16-Jul	31-Jul	13-Aug	
ES+050_LOW	300	1033	1930	1820	1447	1920	1651	919	21	131	504	32	**1951**
ES+050_MARG	1	4	1759	1417	1557	1750	1769	1766	11	353	213	20	**1770**
ES+050_MID	407	1063	1797	1756	1769	1788	1390	733	0	40	28	9	**1797**
ES+050_UP	259	298	1759	1578	1521	1742	1607	1568	107	288	345	124	**1866**
ES+100_LOW	67	206	1189	1179	934	1189	1122	983	0	10	254	0	**1189**
ES+100_MARG	284	1512	1318	768	1015	1238	1335	106	300	850	604	380	**1618**
ES+100_MID	1422	1591	1672	1601	1672	1672	250	81	0	71	0	0	**1672**
ES+140_LOW	110	119	1135	1033	1056	1176	1079	1069	54	156	133	13	**1189**
ES+140_MARG	1447	1631	1631	1529	1570	1631	184	0	0	102	61	0	**1631**
ES+140_MID	1123	1642	1672	1672	1671	1672	550	31	0	0	1	0	**1672**
ES+190_LOW	773	853	1452	1372	1255	1445	680	599	0	81	198	7	**1452**
ES+190_MARG	1103	1279	1279	1279	1279	1279	175	0	0	0	0	0	**1279**
ES+190_MID	1638	1223	1769	1769	1769	1769	132	546	0	0	0	0	**1769**
ES+190_UP	1142	1072	1667	1667	1667	1667	526	595	0	0	0	0	**1667**
Grand Total	**10076**	**13526**	**22029**	**20441**	**20183**	**21939**	**12448**	**8997**	**495**	**2082**	**2340**	**585**	**22524**

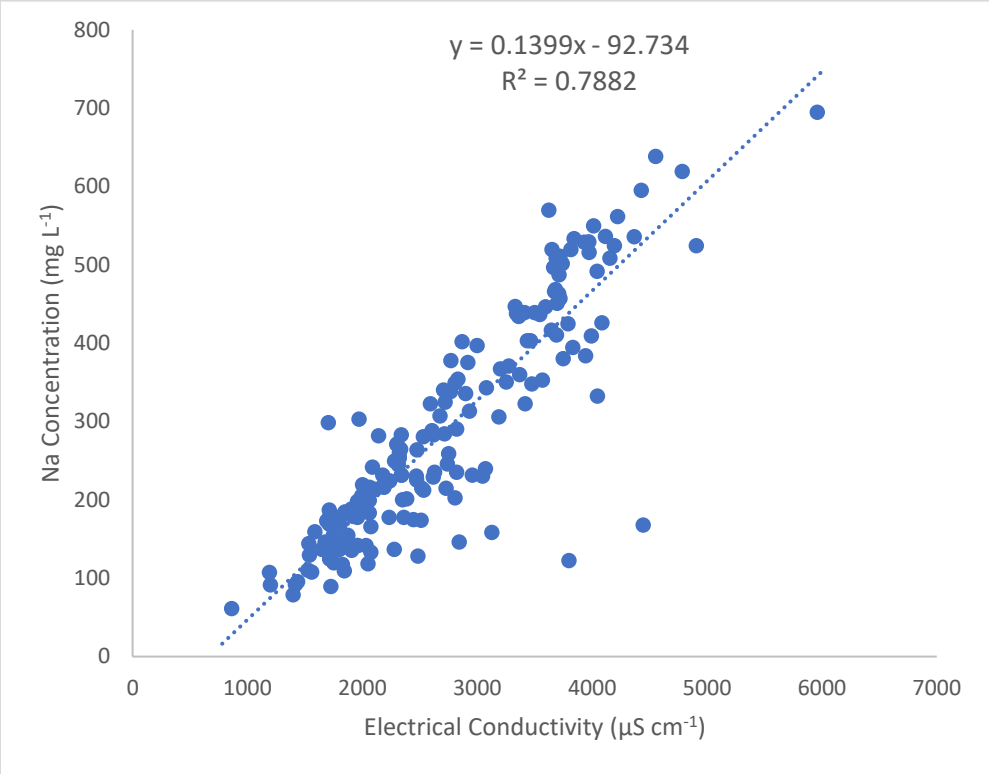

Figure B. 1 Best fit line for Na concentration estimation from EC in surface ponded water samples

Table B. 2 List of adjacent cells of each Na concentration gap-fill required cells.

Gap fill required cells	Adjacent cells
ES+050_LOW	Ave. of 50Mid, 100Low
ES+100_MID	Ave. of 100Low, 50Mid and 140Mid, 50Up
ES+100_MARG	Ave. of 50Marg, 140Marg
ES+190_LOW	Ave. 140Low, 190Mid
ES+190_MARG	Ave. 190Up, 140Marg

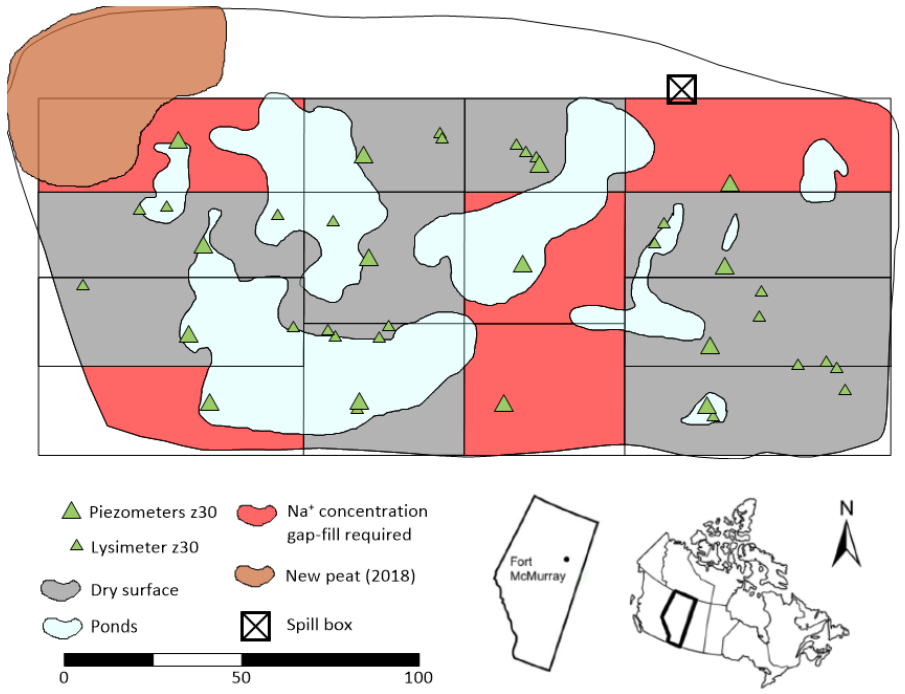

Figure B. 2 Map of the fen with red shaded areas demonstrating the cells that required C_{unsat} gap-fill.

Appendix C

Validation for Na^+ concentrations in discharge

Since HOBO uses a different mechanism than the Orion EC probe, EC measured with HOBO installed at the v-notch was calibrated to EC from water samples collected by the ISCO and then measured with the Orion EC probe, to keep consistency.

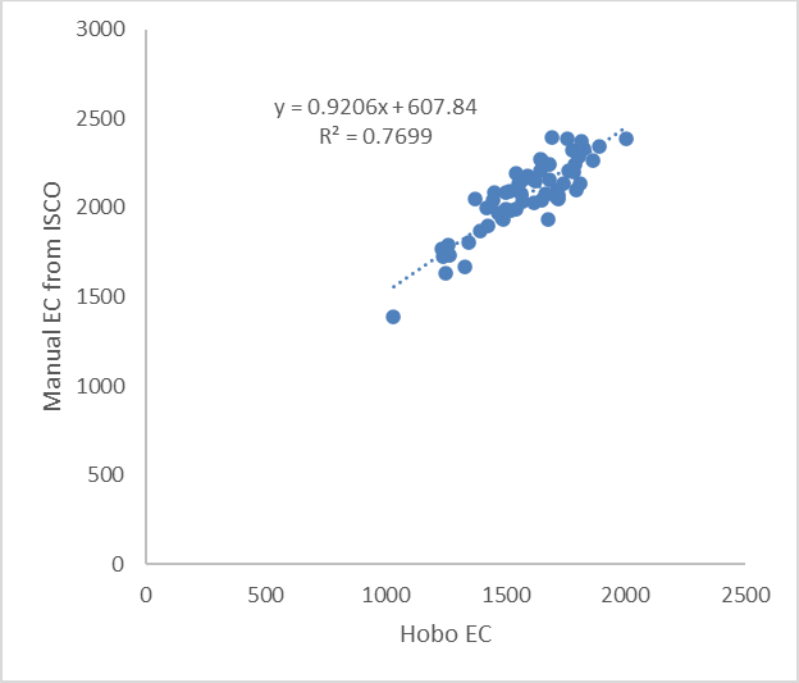

Figure C. 1 Calibration for EC (µS cm^{-1}) measured by HOBO with manual EC measured using ISCO collected water samples.

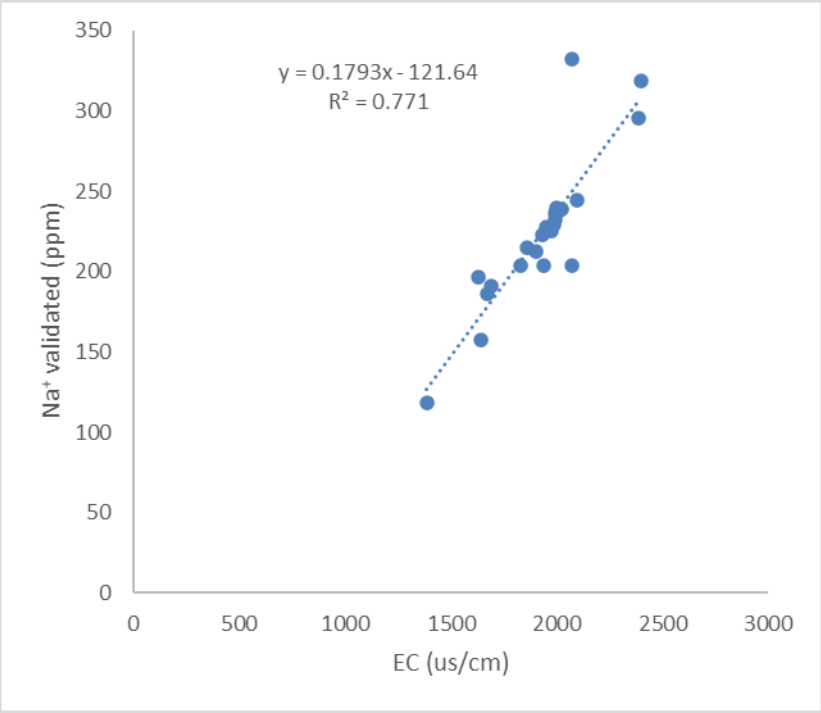

Figure C. 1 Correlation between manual Na^+ concentration (ppm) and EC ($\mu S\ cm^{-1}$) measured in ISCO collected samples. This correlation was used to estimate Na^+ concentration with previously calibrated EC measured by HOBO

Appendix D

Hydrological context in past years

Seasonal precipitation and actual evapotranspiration reported from the eddy covariance system at Nikanotee Fen Watershed between May 18th and August 31st each year from 2013 to 2019 is shown in table below. The average precipitation and mean air temperature reported from Environment Canada at the Fort McMurray airport were 224 mm and 15.4 °C, respectively, between May 18th and August 31st from 1981 to 2018 (Government of Canada, 2020). The average precipitation and the average actual evapotranspiration at Nikanotee Fen Watershed were 212 mm and 330 mm, respectively, between May 18th and August 31st from 2013 to 2018.

Table D. 1 Precipitation (*P*), actual evapotranspiration (*AET*), potential evapotranspiration (*PET*) and temperature (*T*) measured from the eddy covariance system at Nikanotee Fen Watershed between May 18th and August 31st each year from 2013 to 2019.

Year	2013	2014	2015	2016	2017	2018	2019
P (mm)	257	206	140	254	162	253	264
AET (mm)	325	398	423	207	300	326	272
PET (mm)	337	382	392	208	414	375	361
T (°C)	19.1	19.1	15.0	14.9	15.1	14.9	14.0

Appendix E

Calculation process for dilution at ponded surface water

The calculations for fresh water needed to dilute ponded surface water from 461 mg L^{-1} (June 28th) to 181 mg L^{-1} (July 1st) used the following equations. The fresh rainwater would increase the ponded surface water area and thickness (or water level), but for this calculation, it is assumed that the ponded surface area is static.

$$M_1 = C_1 \cdot V_1 \tag{E1}$$

$$M_2 = C_2 \cdot (V_1 + V_d) \tag{E2}$$

$$\Delta M_{water} = M_1 - M_2 \tag{E3}$$

where,

M_1 and M_2 is Na^+ mass estimated in ponded surface water (day 1 and day 2),

C_1 and C_2 is Na^+ concentration in ponded surface water (day 1 and day 2),

V_1 is water volume on day 1,

V_d is estimated freshwater volume added to the ponded surface water area to dilute from C_1 to C_2.

ΔM_{water} is the Na mass storage change in the ponded surface water.

Thus, combining Eq. E1, E2 and E3,

$$V_d = \frac{V_1 \cdot (C_1 - C_2) - \Delta M_{water}}{C_2} \tag{E4}$$

Then V_d/A, where A is the ponded surface water area on day 2, is reported in Chapter 4.1 to compare with the precipitation between June 28th and July 1st (P = 68 mm).

Appendix F

Na^+ mass estimate in peat

In addition to the average Na^+ mass (2705 kg) estimated in the ponded surface water and shallow subsurface peat (0 ~ 35 cm bgs), the Na^+ mass in the deeper peat (35 ~ 200 cm bgs) was calculated using three groundwater sampling events in 2019 to estimate the total Na^+ mass in the fen peat (0 ~ 200 cm bgs) and ponded surface water.

For each cell on each groundwater sampling date, the Na^+ mass in fen peat (35 ~ 200 cm bgs) was calculated using:

$$Na_{peat} = A_{peat} \cdot b_{peat} \cdot C_{peat} \cdot \theta$$

where,

A_{peat} is the peat area, same as the total cell area in mass balance.

b_{peat} is 1.65 m as the thickness.

C_{peat} is average Na concentration measured from groundwater sampling at level 50, 90 and 150 cm bgs with 20 cm slotted intake length. There were 4 cells missing C_{peat}, which was gap-filled using adjacent cells.

θ is the average of volumetric water content of the peat, which being saturated was assumed to equal the porosity of the peat (0.92).

The total of 14 cell on each date would be the Na^+ mass in fen peat (35 ~ 200 cm bgs). The estimated Na^+ mass in the fen peat (0 ~ 200 cm bgs) and ponded surface water was calculated by adding the average from three groundwater sampling events Na_{peat} = 6085 kg with the average Na_{Tot} = 2705 kg as reported in Table 3-5, which was 8791 kg. If excluding the Na^+ mass in ponded surface water, the estimated Na^+ mass in fen peat would be 8454 kg.

Appendix G

Additional violin plots with statistical test for each sampling events

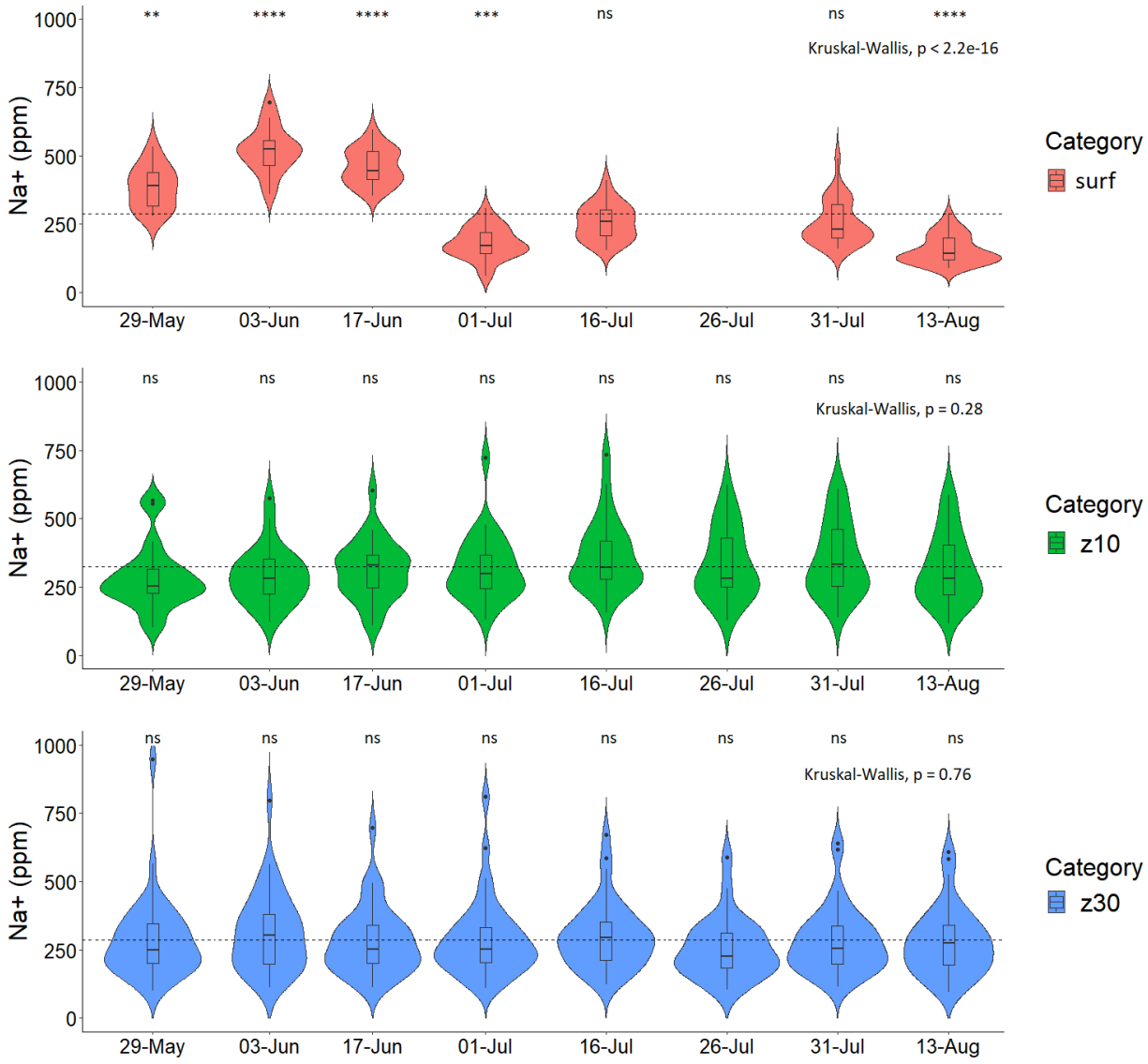

Figure G. 1 Violin plots of Na^+ concentration from each sampling events at surface ponded water (surf), 10 cm bgs (z10) and 30 cm bgs (z30). It included general Kruskal Wallis test p value, and significant level (ns for not significant, *, **, *, and **** indicate significance at 0.05, 0.01, 0.001 and 0.0001, respectively) of each sampling events mean with the general mean (dashed line) for each category (surf, z10 or z30).**

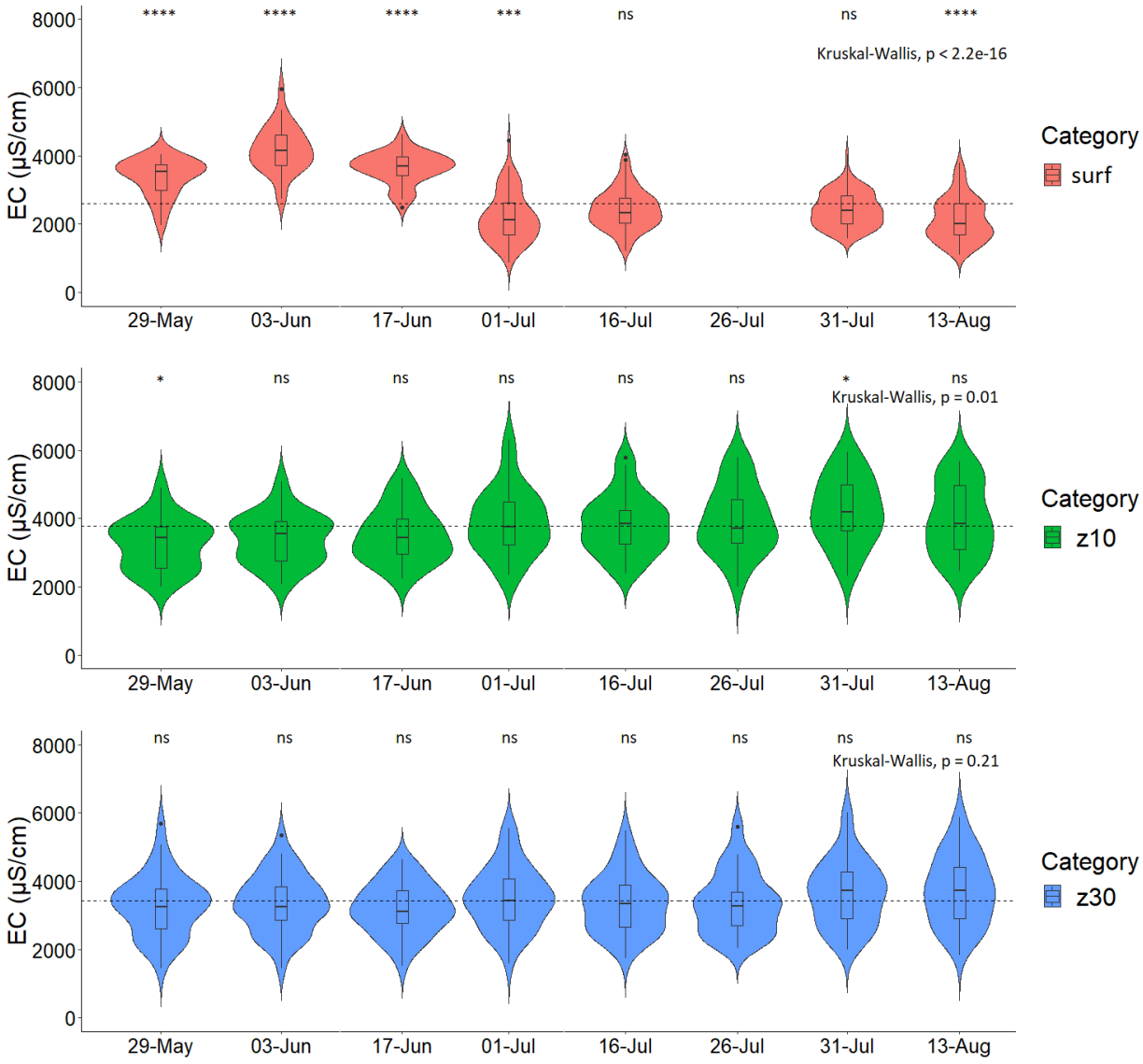

Figure G. 2 Violin plots of EC from each sampling events at surface ponded water (surf), 10 cm bgs (z10) and 30 cm bgs (z30). It included general Kruskal Wallis test p value, and significant level (ns for not significant, *, **, *, and **** indicate significance at 0.05, 0.01, 0.001 and 0.0001, respectively) of each sampling events mean with the general mean (dashed line) for each category (surf, z10 or z30).**

Appendix H

Limitations and gap-fills for groundwater inflow of Na^+ estimation

Na^+ concentration from piezometers centered at 50 cm bgs were only measured once every month (June, July, and August, in total of 3 rounds of sampling) from 10 nests. Thus, cells that were missing Na^+ concentration measurement at 50 cm bgs were gap-filled using the average from adjacent cells on the same date. Na^+ concentration from piezometers centered at 30 cm bgs were sampled a total of 6 rounds including 14 cells each round.

Water level data for i_{vert} were measured in a total of 8 rounds of sampling from June to August. 4 out of 108 well water level data were missing due to ice; these were gap-filled using the average from the closest date in the same cell (e.g., 100-Marg was missing well water level on Jun 11th, gap-filled with average of well water level in 100-Marg on Jun 1st and 25th). There were 4 out of 108 petroleum coke water level measurements (piezometer centered at 225 cm bgs with 20 cm intake) missing. There were 2 measurements from 100-Low missing (on June 1st and June 11th); these were gap-filled with the average from adjacent cells on the same date. Also, 2 were gap-filled using average from the closest date in the same cell. Wells in a few nests (e.g., ES+190-Up) were frozen or filled with snow water in June, thus, they were adjusted with values from adjacent cells.

Since the sampling dates varied in each component in the equations. The date selection for each data follows the table below to match with the mass balance for change in storage. Note that the Na mass calculated by change in storage was from Jun 3rd to Aug 13th.

M_GW date range	Duration	**i 225-w**	**C_GW (z30)**	**C_GW (z50)**
03-Jun to 17-Jun	15	11-Jun	ave of 03-Jun & 17-Jun	28-Jun
18-Jun to 01-Jul	14	ave of 25-Jun & 1-Jul	01-Jul	28-Jun
02-Jul to 16-Jul	15	ave of 04-Jul & 11-Jul	16-Jul	23-Jul
17-Jul to 31-Jul	15	01-Aug	31-Jul	23-Jul
01-Aug to 13-Aug	13	08-Aug	13-Aug	12-Aug

Appendix I

Vertical hydraulic gradient

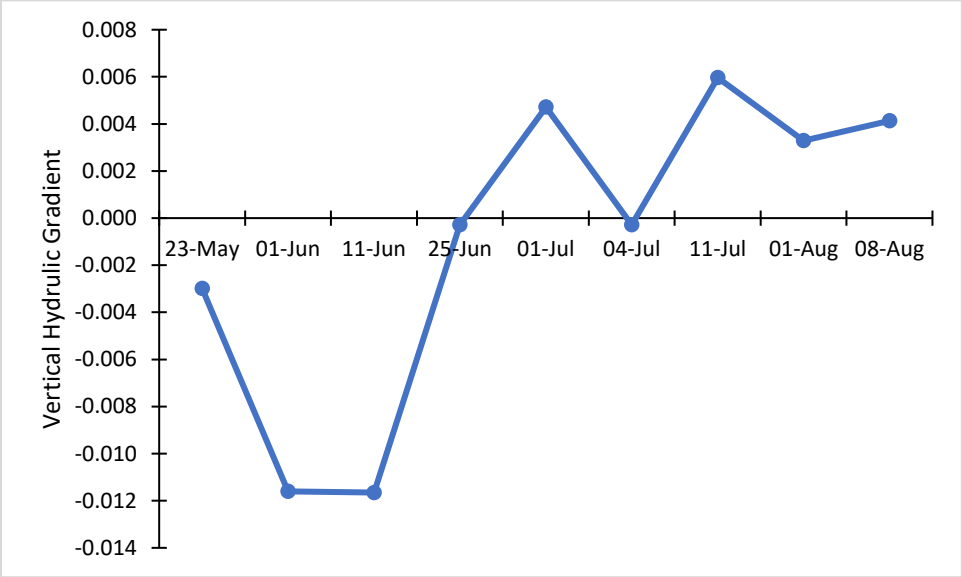

Figure I. 1 Daily average of vertical hydraulic gradient in the fen